

# Magnetic hydroxyapatite nanocomposites: The advances from synthesis to biomedical applications



Asim Mushtaq<sup>a,b</sup>, Ruibo Zhao<sup>a,b</sup>, Dandan Luo<sup>a,b</sup>, Eithne Dempsey<sup>c</sup>, Xiumei Wang<sup>d</sup>, M. Zubair Iqbal<sup>a,b,\*</sup>, Xiangdong Kong<sup>a,b,\*</sup>

<sup>a</sup> Institute of Smart Biomedical Materials, School of Materials Science and Engineering, Zhejiang Sci-Tech University, Hangzhou 310018, China

<sup>b</sup> Zhejiang-Mauritius Joint Research Center for Biomaterials and Tissue Engineering, Hangzhou 310018, China

<sup>c</sup> Department of Chemistry, Kathleen Lonsdale Institute for Human Health Research, Maynooth University, Maynooth, Ireland

<sup>d</sup> State Key Laboratory of New Ceramic & Fine Processing, School of Materials Science and Engineering, Tsinghua University, Beijing 100084, China

## HIGHLIGHTS

- Discussion of the recent progress in synthesis of magnetic hydroxyapatite hybrid nanoparticles.
- Comprehensive assessment on the synthesis of MHAp NCs by various preparation methods.
- Showcasing the remarkable biomedical applications achieved by the magnetic hydroxyapatite NCs.
- Providing insights into the future perspectives of MHAp NCs for Biomedical applications.

## GRAPHICAL ABSTRACT



## ARTICLE INFO

### Article history:

Received 29 July 2020

Received in revised form 11 September 2020

Accepted 24 October 2020

Available online 28 October 2020

### Keywords:

Magnetic nanoparticles

Hydroxyapatite

Nanocomposites

Synthesis techniques

Drug delivery

Tissue engineering

Biomedical applications

## ABSTRACT

Nanoscale materials continue to amaze researchers due to their fascinating versatile properties. One such inspiring development in nanomaterials is the design of the nanocomposite materials for multifunctional purposes from energy storage to biomedical applications. Magnetic hydroxyapatite [MHAp] nanoparticles have achieved considerable attention during the last two decades and possess exceptional prospects in the field of nanomedicine with improved multi-therapeutic approaches. The progress from controlled fabrication to advanced applications of MHAp nanocomposites is still in its infancy and few efforts have been devoted to this cause. The hybrid structure of MHAp is anticipated to be an auspicious platform for biomedical applications particularly in cancer theranostics because of good stability and biocompatibility. In this review, recent exciting features in the development of MHAp nanocomposite and promising applications in controlled drug/gene delivery and magnetic hyperthermia treatment, tissue engineering and bone regeneration, antimicrobial activity, heavy metals and toxic dyes removal, fire retardant behaviour, biosensors and the development of contrast agents for magnetic resonance imaging are highlighted and explained in detail. In addition, this study provides a comprehensive assessment of the synthesis of MHAp nanocomposites by various preparation methods, the influence of reaction parameters on the morphology and structure-property relationships based on recent studies. Finally, novel perceptions are examined regarding the ability of MHAp nanoparticles to improve hybrid nanocarriers with homogeneous structure to enhance multifunctional biomedical applications.

\* Corresponding authors at: Institute of Smart Biomedical Materials, School of Materials Science and Engineering, Zhejiang Sci-Tech University, Hangzhou 310018, China. E-mail addresses: [zubair@zstu.edu.cn](mailto:zubair@zstu.edu.cn) (M.Z. Iqbal), [kongxd@zstu.edu.cn](mailto:kongxd@zstu.edu.cn) (X. Kong).

## 1. Introduction

Magnetic nano-materials have been valuable for catalysis [1], colloidal photonic crystals [2], magnetic particle imaging [3], nanofluids [4], data storage [5], defect sensor [6], optical filters [7], and environmental remediation [8]. Particularly, magnetic nanoparticles have potential use in the biomedical industry because of their unique mechanical, thermal, physical and chemical properties [9]. The most commonly used magnetic materials are based on iron, manganese, nickel, gadolinium, cobalt, and their components. The oxides of iron, manganese and gadolinium have attained significant interest in biomedical imaging owing to their externally magnetic manipulated behaviour and low toxicity [10,11]. Due to the fascinating properties of magnetic nanoparticles, they have been utilized in magnetic resonance imaging (MRI), controlled drug delivery to cancer/tumor cells, tissue growth, cell separation, molecular labeling and gene delivery [12,13]. The magnetic materials used in biomedical research possess some advantages and disadvantages. For example, magnetic materials having Gd, Sm and Nd require high external field and controlled environment for their propagation. It is a fact that magnetic materials give remarkable results for cancer diagnosis and controlled drug delivery applications. However, some magnetic based nanocomposites may not be directly applicable because of toxicity concerns. Therefore, surface modification with biocompatible materials or polymers is used to reduce the toxicity and facilitate the coating of secondary materials onto the surface of these magnetic nanocomposites (MNCs).

Hydroxyapatite (HAp) is a highly biocompatible calcium and phosphorus containing bio ceramic material that has the same element ratio (Ca:P  $\approx$  1.67) as natural bones and teeth. Because of bioactivity, osteo-inductive capability, non-immunogenic behaviour, diversity in shapes and biodegradability, HAp has aroused extensive interest for biomedical applications [14]. Moreover, HAp has surface phenomena with ion exchange and adsorption properties that leads to doping, grafting and loading processes. Owing to the advancement in nanotechnology, scientists have made great efforts to produce new morphologies of HAp for the expansion of the HAp family and its applications [15].

Recently, researchers have paid much attention to the design of composite nanostructures by mixing two or more components to synthesize a single nano-system which delivers enhanced multifunctional properties because of its colloidal nature. The ability to prepare a variety of composite nanomaterials is totally dependent on the physiochemical, external and internal interfacial properties of individual components. Nanocomposite (NC) materials are widely used in high power batteries, lightweight sensors, conductive paper for flexible batteries and the healing process of bones [16]. Therefore, it is a promising research area to fabricate NCs for multi-purposes. However, it is always a challenge to design NCs with expected homogeneous size and controlled structure especially at the nanoscale. Meanwhile, the selection of materials is also crucial to attain the desired properties for different application. Consequently, researchers are working on integrating magnetic nanoparticles with other biocompatible materials (HAp) for enhanced multifunctional applications. Another important factor involved in the design of NCs is lattice geometry distribution. Some regular structures such as core-shell composites have a centrosymmetric structure and it is usually observed that the hybrid nanostructures are formed at same lattice constants. Generally, lattice (matched/mismatched) experiences considerable geometry distributions which are much sophisticated to keep it restrain. Furthermore, the surface of these NCs is modified with biodegradable materials for improvement of their synergetic properties.

Interestingly, the physiochemical nature of HAp facilitates other species to establish composites with it [17]. On the other hand, magnetic

nanoparticles have the ability to join with various kinds of proteins, specific enzymes, targeted drugs and many antibodies. Therefore, the integration of these two promising materials to design nanocomposites will open a novel platform in the field of nano-biotechnology. Also, the distinct surface features provide multiple coatings such as antitumor and anti-inflammatory agents and in tissue culturing [18]. Special shaped structures (core-shell, liposomes, dumbbell) have the ability to improve the functions and properties of nanomaterials. The properties like catalytic activity, thermal stability, pH sensitivity, optical and magnetic behaviour depends upon the composites/core-shell materials. Furthermore, these properties can be tunable by controlling the thickness, size and shape of core-shell structures. In a true sense composites/core-shells represent materials having two kinds of properties in one system. By increasing the number of materials in composites, the properties may be altered and improved. So, there is a wide range of biological features depending upon the type of magnetic nanoparticles and composites/core-shells [19]. For example, if we use the  $\text{Fe}_3\text{O}_4$  magnetic nanoparticles and coat them with two different materials, such as silica and ethylene glycol then these particles will represent the three types of properties - magnetic properties, drug carrier agent and optical properties [20]. There are various kinds of polymeric materials used for surface modifications to design shells or to stabilize magnetic-HAp NPs, e.g. chitosan, dextran, N-(phosphonomethyl)-iminodiacetic acid (PM-IDA), Poly (vinyl) alcohol (PVA), poly-ethylenimine, poly-ethylene glycol, and silica [18].

In this review, recent advances in the use of magnetic HAp NCs as a potential candidate for biomedical applications are reported. A variety of synthetic approaches will be discussed and compared to develop better understanding about how the size, shape, and crystal structure of these NCs can be controlled. This review will also discuss the biocompatibility and improvements in biomedical applications of magnetic HAp NCs in view of emerging challenges and modifications.

## 2. Synthesis of magnetic HAp nanocomposites

A variety of synthetic approaches was employed to design magneto HAp NCs. The fabrication methods involve hydro/solvothermal method, mechanochemical method, chemical precipitation methods including coprecipitation and wet precipitation, ion exchange method, template method and emulsion synthesis methods. Each method represents unique and significant influence on morphologies, crystalline structure, shape and size of the magnetic HAp NCs. The details are discussed below and are summarized in Table 1.

### 2.1. Hydrothermal method

This is a common method for the synthesis of stoichiometrically regular and crystalline nanoparticles. In this fabrication process, the reactant mixture is poured in the autoclave having a high pressure and temperature environment.

There are many advantages of the hydrothermal method over conventional as well as nonconventional systems. It is a cost effective, easy and environmentally friendly technique. Moreover, the variety of particle size and morphologies are an additional outcome of hydrothermal processes. Likewise, this method gives the final product in solution form which is required for biomedical applications. A foremost advantage of this technique is the hybridization with other techniques like ultrasound, microwaves, optical radiation, hot-pressing, electrochemistry, and mechanochemistry.

Multifunctional magnetic HAp microspheres of  $\text{CaCO}_3/\text{Fe}_3\text{O}_4$  were prepared with open macropores size of 50–200 nm. There was the

**Table 1**  
Summary of different synthetic methods of magnetic HAp nanocomposites along with applications.

| Sr # | Synthetic Route               | Material  | Application   | Advantage   | Disadvantage   | Ref.        |
|------|-------------------------------|---|---|---|--|-------------|
| 1    | Hydrothermal method           | CaCO <sub>3</sub> /Fe <sub>3</sub> O <sub>4</sub> -HAp, Fe <sub>3</sub> O <sub>4</sub> -HAp, Co-HAp, Gd doped HAp                           | Bone regeneration, Antimicrobial, Drug delivery, Hyperthermia, MRI                      | Homogeneous crystal growth, large scale synthesis                           | Seed crystallization, uncontrolled Growth  | 21–24, 27.  |
| 2    | Chemical Precipitation method | Fe/Sr-HAp, Fe <sub>2</sub> O <sub>3</sub> @HAp, lanthanum-doped HA/CS, Fe <sub>3</sub> O <sub>4</sub> /SiO <sub>2</sub> -HAp                | Bone regeneration, Tissue engineering, Magnetic Hyperthermia, Cell study, Drug delivery | High degree of selectivity, Suitable for core-shell structures              | Formation of silt and by products  | 32–35, 39.  |
| 3    | Mechanochemical method        | HAp/MgTiO <sub>3</sub> -MgO, HAp/Fe <sub>3</sub> O <sub>4</sub> .   | Magnetic Hyperthermia   | Suitable for production of powder materials, Solvent free synthesis         | Chance of inhomogeneity, induced de-mixing while agitation   | 48, 51, 52. |
| 4    | Emulsion method               | Fe <sub>3</sub> O <sub>4</sub> -HAp, HAp@ CoFe <sub>2</sub> O <sub>4</sub> , Fe-HAp   | Heavy metals and dyes removal, Tissue engineering                                       | Appropriate for synthesis of microbeads, microsphere, Rapid poly-merization | Reaction of emulsifier leading to poor clarity   | 53–55       |
| 5    | Template method               | CoFe <sub>2</sub> O <sub>4</sub> / SiO <sub>2</sub> -HAp, Iron/HAp, Fe <sub>3</sub> O <sub>4</sub> or MnFe <sub>3</sub> O <sub>4</sub> -HAp | Drug delivery, Fluorescence Sensors   | Controlled size and morphology  | Cracking and defects in products are possible while the removal of hard templates, less stability of soft template | 58, 59, 62  |
| 6    | Synergistic method            | chitosan/collagen/Fe <sub>3</sub> O <sub>4</sub> -nHAp, Fe <sub>2</sub> O <sub>3</sub> @HAp-Ag  | Antioxidant & Anti-inflammatory, Catalysis  | Useful to improve the morphology and crystalline structure of nanomaterial  | Applicable for limited materials   | 66, 67      |

formation of CaCO<sub>3</sub>/Fe<sub>3</sub>O<sub>4</sub> microspheres (Fig. 1 a, b) then transformation to magnetic HAp microspheres (Fig. 1 c-e). Due to the dispersion of Fe<sub>3</sub>O<sub>4</sub> particles in the microsphere, the material had good magnetic strength with 3.98 emug<sup>-1</sup>. Results proved the biocompatibility, drug delivery and antibacterial behaviour of magnetic HAp microspheres [21]. Sahoo et al. reported the synthesis of magnetic HAp nanoparticles for the removal of Eriochrome black T (EBT) in an aqueous medium. The magnetic part of hexagonal particles of Fe<sub>3</sub>O<sub>4</sub> was about 20 nm to 50 nm [22]. Zhuang and coworkers synthesized monodisperse microspheres of Fe<sub>3</sub>O<sub>4</sub>/HAp NCs for lead(II) removal by giving 440 mg/g sorption in 1 h at 3.0 acidic pH [23]. Sarath Chandra et al. synthesized magneto HAp nanoparticles by a hydrothermal method assisted with microwave and the products presented strong magnetic properties due to the magnetic ions (Ni, Co, Fe). The special feature of Co<sup>+2</sup> in Co-HAp was the change of morphology of monodispersed spheres from spherical to

hexagonal rods with superparamagnetic properties. The size of the monodispersed microspheres was 121 nm. By the addition of Co<sup>+2</sup>, there was an increase in magnetic moment from 1.2 × 10<sup>-2</sup> to 6.1 × 10<sup>-2</sup> emug<sup>-1</sup> with the value of dielectric constant 1–2476 [24]. In other work, HAp and Co-HAp powder was prepared. Morphology and cell parameters were checked by known analytical techniques and SEM results proved that there was an increase in the size of HAp nanoparticles due to combination of Co [25]. Chen and co-workers fabricated the magneto HAp nanorods and the nucleation rate of HAp nanocrystals was improved by Fe<sub>3</sub>O<sub>4</sub> coating up to 3 days after the reaction. Furthermore, the biocompatibility was also checked [26].

Liu et al. worked on the HAp nanorods doped by gadolinium, having magnetic resonance relaxation rate r<sub>1</sub> value 5.49 s<sup>-1</sup>(mm)<sup>-1</sup> as shown in Fig. 2 (a). The diameter and length of HAp-Gd nanorods were 9.2 ± 2.4 nm and 29.1 ± 6.2 nm respectively (Fig. 2 (b,c)). Additionally,

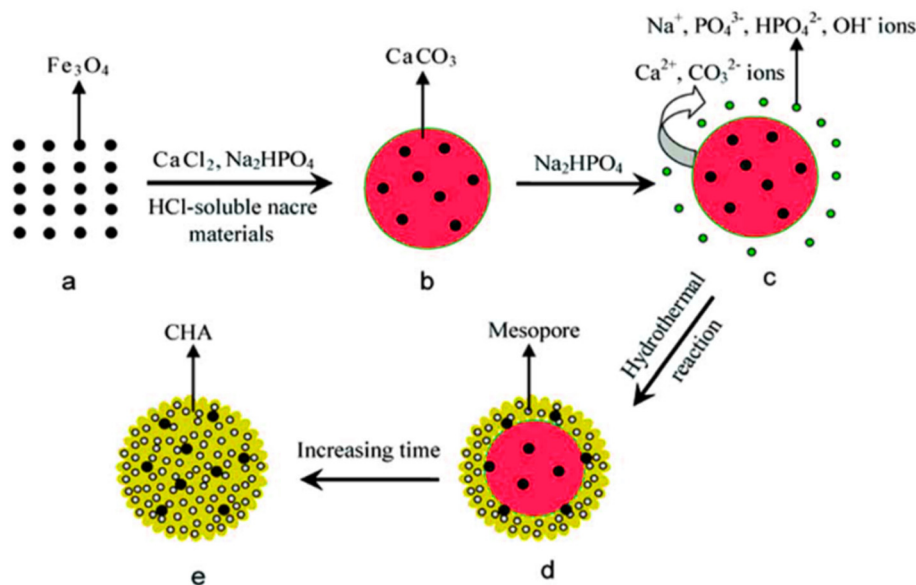


**Fig. 1.** Schematic illustration for the synthesis of magnetic HAp microspheres: (a) Fe<sub>3</sub>O<sub>4</sub> NPs used as magnetic cores; (b) fabrication of CaCO<sub>3</sub>/Fe<sub>3</sub>O<sub>4</sub> microspheres using precipitation method; (c) immersion of CaCO<sub>3</sub>/Fe<sub>3</sub>O<sub>4</sub> microspheres into a Na<sub>2</sub>HPO<sub>4</sub> solution; (d) deposition of CHA nanoparticles (yellow particles) on the surface of microspheres by hydrothermal process, and development of mesopores (white circles) due to the aggregates of CHA nanoparticles; (e) construction of MHMs upon increasing the reaction time. Reprinted with the permission of [21]. Copyright (2014) The Royal Society of Chemistry.

nanorods were excellently dispersed in water having  $-23.7$  mV zeta potential. Furthermore, Sm-153 was post labeled with the *in vitro* stability over 48 h and enhanced the dual-modality imaging *in vivo* for MRI and SPECT [27]. Murakami and co-workers reported the modified hydrothermal synthesis of porous rod-shaped cages of magnetic  $\text{Fe}_3\text{O}_4$ -HAp composites that can hold magnetite by 30 mass%. They blended magnetite particles with the size of  $1 \mu\text{m}$  with poly(L-lactic acid) fibers ( $400 \mu\text{m}$ ). Moreover, temperature bearing ability up to  $55^\circ\text{C}$  within 10 min proved the viability of composites for therapeutic environments under controlled magnetic field [30]. Guo and his team designed mesoporous magneto HAp carbonated microspheres and fabricated  $\text{Fe}_3\text{O}_4/\text{CaCO}_3$  as shown in Fig. 2 (d, e). The pore size of magnetic HAp microspheres was  $3.6\text{--}14.6$  nm (Fig. 2 (f)). Moreover, magnetic properties, hexagonal crystal growth and crystal orientation was influenced by  $\text{Fe}_3\text{O}_4$  [28].

Periyasamy et al. formed magneto HAp alginate beads with good sorptive ability and sorption behaviour of these  $\text{Fe}_3\text{O}_4@n\text{-HApAlg}$  beads was studied by Dubinin-Radushkevich (D-R), Langmuir and Freundlich isotherms. The kinetic study gave pseudo-first and

pseudo-second-order data. These beads proved to be re-useable up to 5 times by the use of NaOH eluent [31]. In another study, biocompatible and pH-sensitive hierarchically mesoporous magnetic HAp hollow microspheres were synthesized resulting in  $20$  nm  $\text{Fe}_3\text{O}_4$  magnetic particles. The average size of  $\text{CaCO}_3/\text{Fe}_3\text{O}_4$  hollow microspheres was  $0.75\text{--}0.96 \mu\text{m}$ . The magnetic properties of composites were controlled by the amount of  $\text{Fe}_3\text{O}_4$ . As compared to the HAp particles, the magnetic and modified HAp composites presented excellent therapeutic and biocompatible features [29].

The above reports demonstrate promising control over rod and hollow shaped morphology with additional surface functionalities of magnetic particles to link drugs and biomolecules. This method is also favorable for large scale synthesis of magnetic HAp NCs.

## 2.2. Chemical precipitation method

This is an easy method to control the composition, size of nanomaterials, and useful for the preparation of homogeneous particles as well as surface modification. Various potential morphologies of

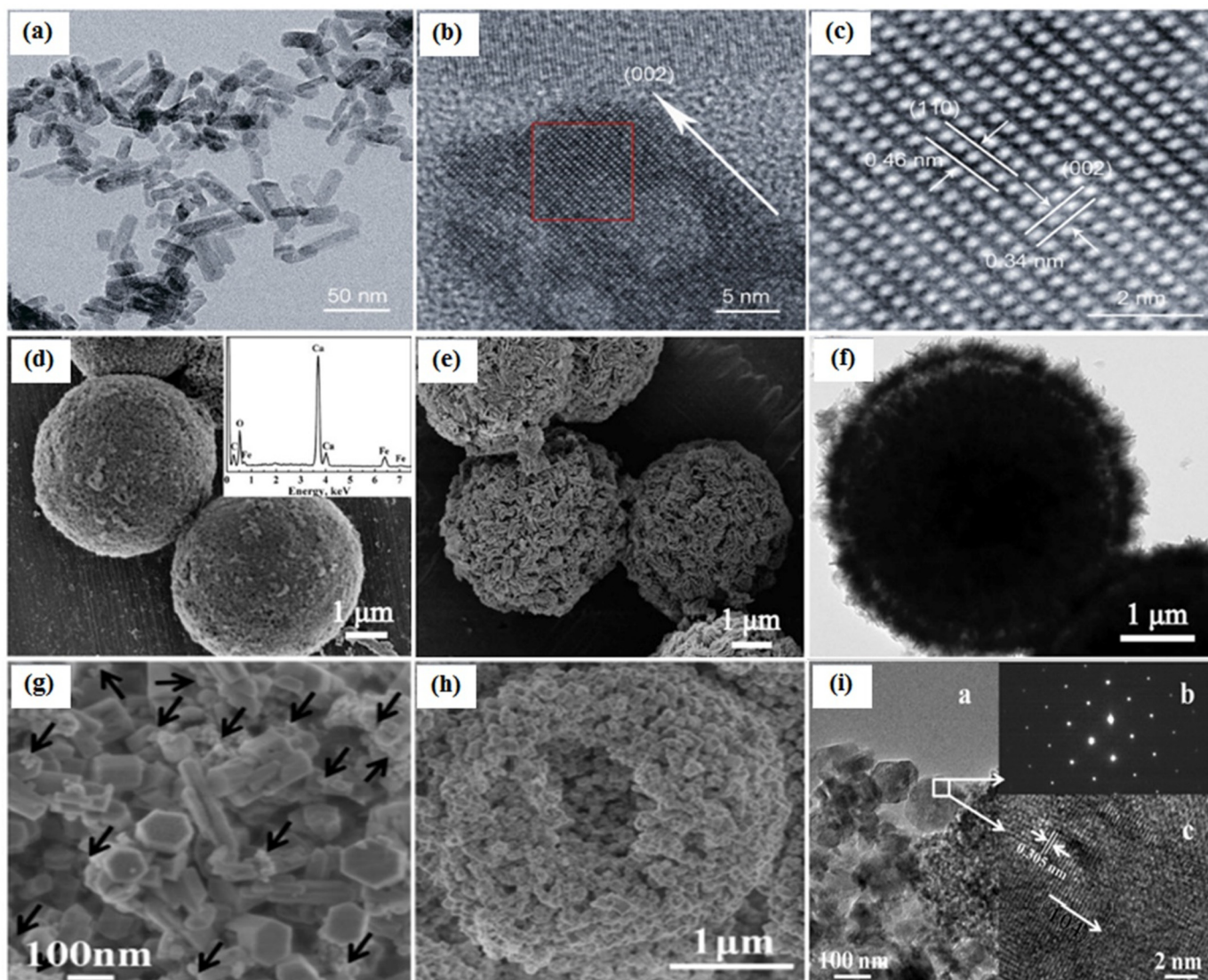


**Fig. 2.** (a) TEM image of  $\text{Cd}^{3+}$  doped magnetic hydroxyapatite nanorods; (b) HR-TEM images of magnetic HAp nanorods; (c) Crystal lattice pattern of magnetic HAp nanorods. Reprinted with the permission of [27]. Copyright (2013) Elsevier Ltd. (d) SEM image of  $\text{CaCO}_3/\text{Fe}_3\text{O}_4$ -HAp microspheres; (e) SEM image of magnetic carbonated HAp microspheres; (f) TEM image of  $\text{CaCO}_3/\text{Fe}_3\text{O}_4$ -HAp microspheres. Reprinted with the permission of [28]. Copyright (2011) The Royal Society of Chemistry. (g) High magnification image of  $\text{CaCO}_3/\text{Fe}_3\text{O}_4$ -HAp hollow microspheres; (h) SEM image of  $\text{CaCO}_3/\text{Fe}_3\text{O}_4$ -HAp hollow microspheres; (i) a. TEM, b. SAED, and c. HRTEM images of single particle taken from  $\text{CaCO}_3/\text{Fe}_3\text{O}_4$ -HAp hollow microspheres. Reprinted with the permission of [29]. Copyright (2013) The Royal Society of Chemistry.

magnetic-HAp NCs were synthesized and some excellent studies are described hereafter.

Ullah et al. followed the aqueous chemical precipitation method with sonication assistance to make Fe/Sr co-doped HAp bionanomaterials. The size of particles was 140–205 nm, surface area  $186 \text{ m}^2\text{g}^{-1}$  and pore size about 13–19 nm, representing relatively negative zeta value at 7 pH. The thermal phase stability was shown to be lowered by the substitution of  $\text{Fe}^{3+}$  in HAp as compared to the pure HAp and Sr-HAp. Additionally, co-doping of  $\text{Fe}^{3+}$  and  $\text{Sr}^{2+}$  imparted a synergistic effect in improvement of alkaline phosphatase (ALP) activity and calcium deposition [32]. In other work by same group, they reported Fe/Sr modified HAp bioceramic composites and their biological activities were checked by acid citrate dextrose (ACD) test for *in vitro* blood compatibility, alkaline phosphatase test for osteoblastic cell differentiation, and *in vitro* drug loading and release analysis resulted the justification of NCs biocompatibility. The morphological study presented structures of  $0.8 \mu\text{m}$  having polyphasic ability by co-substitution of ions. There was a positive change in dielectric constant by the addition of Fe/Sr in HAp. The scheme of study is presented in Fig. 3 [33].

Ramos-guivar and co-workers reported the preparation of magnetic nanoparticles of  $\gamma\text{-Fe}_2\text{O}_3$  embedded into the matrix of nano HAp with 10–20 nm sizes with rod shape morphology as shown in Fig. 4 (a–c), and the corresponding EDX results presented atomic composition associated to  $\gamma\text{-Fe}_2\text{O}_3$  @ HAp (Fig. 4, d). Furthermore, the magnified TEM image (Fig. 4, e) showed the dispersion of  $\gamma\text{-Fe}_2\text{O}_3$  NPs on the matrix of HAp and superparamagnetic behaviour presented in Fig. 4 (f–g). These  $\gamma\text{-Fe}_2\text{O}_3$ /HAp NCs presented no toxicity and were reported to be biocompatible [34].

A study by Qiyang Wang et al. involved the fabrication of bioactive and biocompatible NCs based on magnetic lanthanum-doped hydroxyapatite chitosan (MLHAp@CS). Magnetic  $\text{SrFe}_{12}\text{O}_{19}$  nanoparticles were doped into LHAp/CS and the prepared NCs were in a plate shaped structure with 50–150 nm width and 30 nm thickness. MLHAp@CS NCs scaffolds offered very positive results for bone regeneration without the help

of external growth factors [35]. Adsorption behaviour of HAp/ $\text{Fe}_3\text{O}_4$  nanocomposites was studied by Vahdat et al. with the change in concentration, pH, contact time and temperature. An isothermal and kinetic study was also carried out [36]. A study was reported on the synthesis of  $\text{CuO@HAp@}\gamma\text{-Fe}_2\text{O}_3$  hybrid magnetic nanoparticles via an ion exchange chemical precipitation method. The morphology was revealed to be nanosheets of irregular shapes and various sizes [37].

Xiao et al. used the wet chemical method for the production of magneto HAp nanostructures doped by Fe/ $\gamma\text{-Fe}_2\text{O}_3$ . These magnetic nanostructures showed excellent adsorption properties as compared to other HAp based adsorbents [38]. Other research reported by Mortazavi-Derazkola and co-workers involved preparation of  $\text{Fe}_3\text{O}_4/\text{SiO}_2/\text{HAp}$  NCs by chemical precipitation with the assistance of ultrasonics. The MNCs possessed sphere like morphology with 13.37 nm pore size and  $55.88 \text{ m}^2\text{g}^{-1}$  surface area. Furthermore, the effect of glucose and fructose as a capping agent was also studied and modified by 3-Aminopropyl triethoxy silane [39]. Wakiya et al. synthesized 0.5–3  $\mu\text{m}$  round with dimple shaped magnetic composites of HAp- $\gamma\text{-Fe}_2\text{O}_3/\text{Fe}_3\text{O}_4$  by ultrasonic-assisted coprecipitation. The saturation magnetization of biocompatible composites was  $0.833 \text{ emu g}^{-1}$  [40]. Work by Yang and companions involved the synthesis of superparamagnetic  $\text{Fe}_3\text{O}_4$  into HAp nanoparticles by homogeneous precipitation technique. The morphological study proved the spherical shape with 25 nm diameter [41]. Zuo and the team used a coprecipitation technique for the formation of Fe doped HAp magnetic particles and also studied the effect of temperature and concentration on magnetic property and morphology. Results specified that iron ion doping lowered the crystallinity. The composites with 10% and 50% iron ions were superparamagnetic but with 30% showed little ferromagnetic behaviour [42].

Few studies have reported on the design of core-shell structure of magnetic HAp using a coprecipitation method. Fe/Mn-HAp core-shell structure was reported by Pon-On and co-workers. EDS results justified that nanoparticles were amorphous at  $500^\circ\text{C}$  and become crystalline at  $1000^\circ\text{C}$ . Moreover size was also increased from 10 to 20 nm to approximately 50 nm by the increase in temperature. TEM images proved the

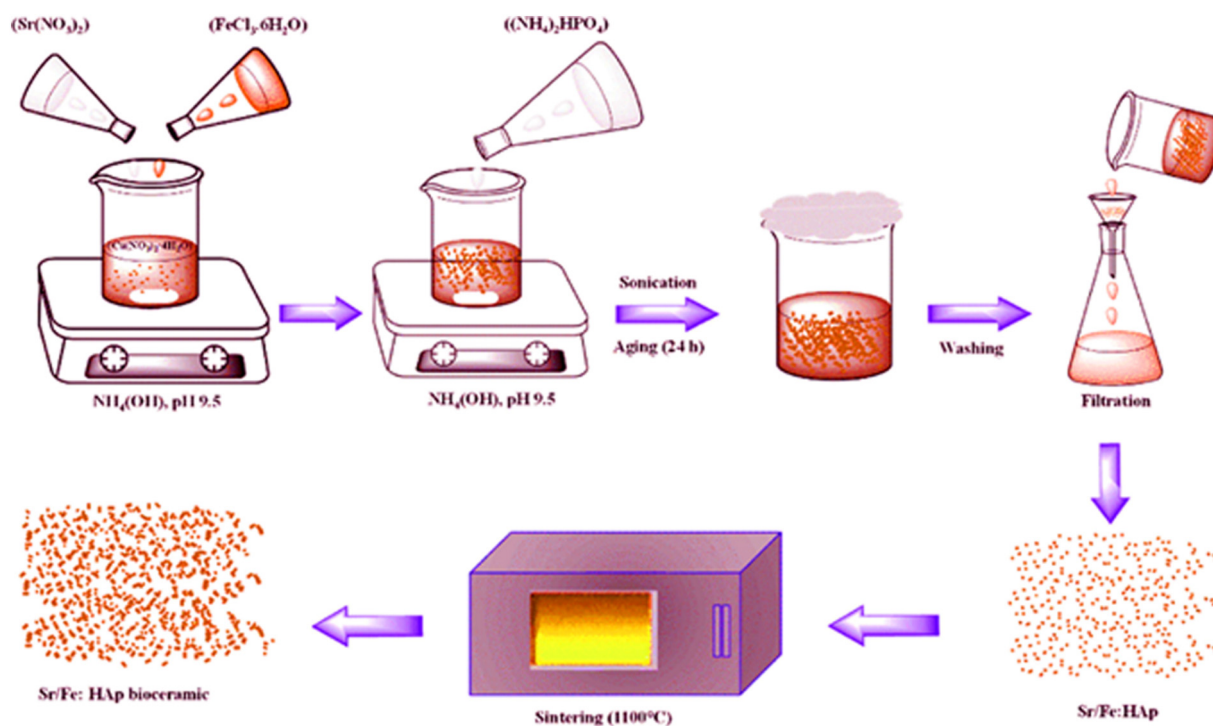
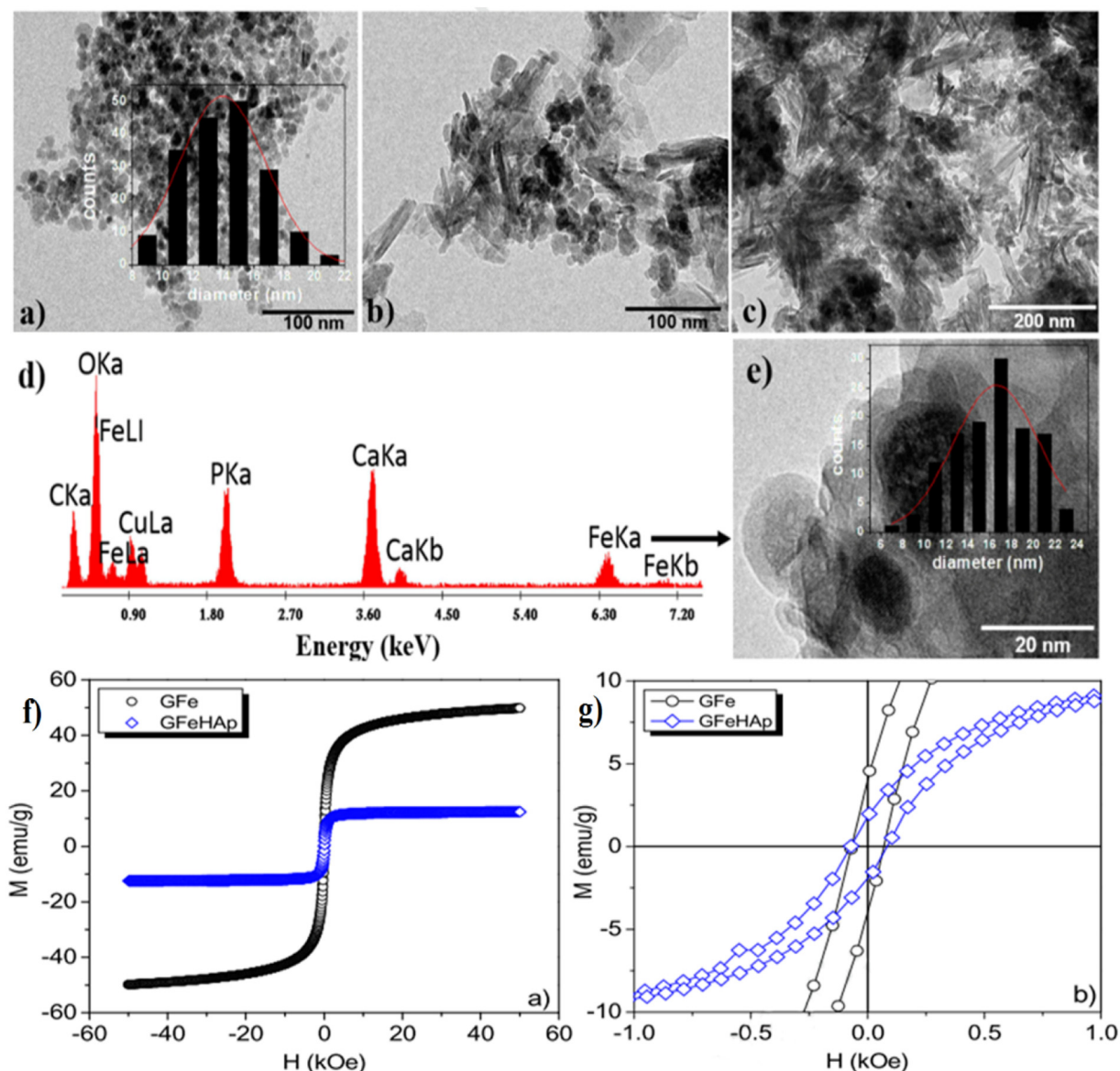


Fig. 3. Schematic presentation for the fabrication of Sr/Fe-HAp bioceramics materials by chemical precipitation method. Reprinted with the permission of [33]. Copyright (2014) The Royal Society of Chemistry.



**Fig. 4.** (a) TEM image of GFe NPs, (b, c, e) TEM images of GFe-HAp NCs, (d) EDX spectra of GFe-HAp NCs and (f, g) magnetic moment M-H loops for GFe and GFe HAp samples at room temperature. Reprinted with the permission of [34]. Copyright (2020) Elsevier Ltd.

core-shell structure of Fe/Mn-HAp. ESR spectroscopy showed  $g$ -factor values 4.23 and 2.01 for  $\text{Fe}^{3+}$  and  $\text{Mn}^{2+}$  respectively and presented that  $\text{Fe}^{3+}$  and  $\text{Mn}^{2+}$  were entered into the  $\text{Ca}^{2+}$  sites of HAp structure [43]. Safaei et al. prepared  $\text{Fe}_3\text{O}_4/\text{HAp}$  core-shell nanostructures and iron oxide particles (26.3 nm) were coated by HAp resulted in rocky material. At high pressure, fluid flow tests were performed and it showed that wettability alteration reduced the pressure drop up to 32%  $\text{Fe}_3\text{O}_4\text{-HAp}/\text{distilled water}$  nanofluid [44]. A study by Petchsang et al. involved the synthesis of 90 nm size cobalt-iron doped HAp core-shell structures. These particles had a HAp shell and  $\text{CoFe}_2\text{O}_4$  core. A decrease of saturation magnetization was reported by the increase in the doping level [45].

The outcomes from chemical precipitation method exhibited the effectiveness of the process. In the core-shell synthesis, this method represents significant results and in most of the cases the magnetic core was covered by HAp shell. It is also observed that the formation of core-shell depends upon the stirring time, temperature, and concentration of materials. Moreover, modifications like ultrasonics, temperature

assistance, wet method, and ion exchange offered virtuous effects to control the morphology and size of NCs.

### 2.3. Mechanochemical method

Many nanomaterials are formed by a dry/solvent-free or liquid assisted method called a mechanochemical method. Mechanochemical synthesis is environmentally friendly, low cost and very simple operational technology [46]. This method is also used to prepare a variety of heterogeneous nanoparticles and important variables such as precursors, speed, time and milling medium used while grinding of material for mechanochemical method are important. If milling is solvent-free then it is called a dry method and if milling is solvent assisted then it is called a wet method. In the wet mechanochemical method a very small amount of solvent is utilized [47].

Fahami et al. synthesized NCs of HAp-20%wt Ti and ellipse like powder was formed after milling for 20 h at 650 °C,  $25 \pm 15$  nm [49]. In another work, they followed the mechanochemical method for 10 h with

thermal assistance of 700 °C for the production of HAp/MgTiO<sub>3</sub>-MgO nanopowder having 21 and 34 nm crystallite size. Furthermore, HAp decomposition into tricalcium phosphate was also studied with the change of temperature from 900 °C to 1100 °C and nanopowder of β-TCP/ MgTiO<sub>3</sub>-MgO formed [50]. Later, Fahami and Nasiri-Tabrizi developed the mechano-thermal technique for the preparation of HAp/MgTiO<sub>3</sub>-MgO NCs powder with large agglomerates and spheroidal morphology. Crystallite sizes were the same as in previous work (21 nm and 34 nm). This composite powder was obtained by milling for 10 h at 700 °C as presented in scheme of study (Fig. 5) [48].

Iwasaki developed a simple mechanochemical method for the formation of HAp/Fe<sub>3</sub>O<sub>4</sub> NCs. The synthesized material was investigated morphologically, thermodynamically, magnetically and biologically. Highly crystalline 16 nm median diameter Fe<sub>3</sub>O<sub>4</sub> particles showed super-paramagnetic behaviour with magnetization of 78 emug<sup>-1</sup> (Fig. 6) [51]. Sneha and Sundaram prepared superparamagnetic and biocompatible NCs of HAp/Fe<sub>3</sub>O<sub>4</sub> with ratio of 1.5:1 (w/w) by wet mechanochemical method at 300 rpm for 5 h. The morphology of particles was spherical shape with size of 100–350 nm [52].

The mechanochemical method proved to be very useful for the synthesis of magnetic HAp nanopowders. Moreover, high crystallinity of particles was also observed. The mechanochemical method is limited for magnetic HAp production due to non-homogeneous structures, aggregation, and time involved.

#### 2.4. Emulsion synthesis method

In the emulsion synthesis method, microemulsions are formed with specific parameters like controlled size, specific morphology and low aggregation of nanomaterials. The emulsion method is considered to be safe as no high-pressure conditions are required. Microemulsions are formed by two immiscible phases like water and oil, and stabilization is achieved *via* surfactants. In this regard, Foroughi and co-workers prepared nanopowders of CoFe<sub>2</sub>O<sub>4</sub> having core-shell of HAp at 700 °C and core-shell morphology was confirmed by TEM. Maximum magnetism was shown 7.8 emug<sup>-1</sup> and it was decreased by changing the temperature from 700 °C–900 °C. The reason for the decrease in magnetic power was the reaction between CoFe<sub>2</sub>O<sub>4</sub> and HAp [54]. In another work Zhang et al. synthesized microbeads of magnetic HAp/agar NCs and the magnetic moiety was Fe<sub>3</sub>O<sub>4</sub> having surface modification with phosphonomethyl iminoacetic acid. According to the morphology, these beads were 150 μm spherical with a surface area of 90 m<sup>2</sup>g<sup>-1</sup> (Fig. 7). Furthermore, these superparamagnetic large size microbeads had more adsorption ability [53]. Iafisco et al. formed the hollow magnetic FeHAp nano-microspheres having size 500 nm–2 μm using hybrid polymeric materials like poly L-lactic acid and CH<sub>2</sub>Cl<sub>2</sub> as an emulsifier. The physical and chemical features of spheres were controlled by the concentration of FeHAp. These microspheres showed good biocompatibility. The time for the formation of microspheres from dichloromethane emulsion was 3 days at the temperature of 30 °C [55].

This technique realises formation of magnetic HAp microbeads, coreshells and microspheres with low aggregation of materials under low pressure and temperature conditions.

#### 2.5. Template method

The template method is a new material fabrication strategy and has gain attraction in recent years with control of the structure, morphology and particle size of nanomaterials [56,57].

For the preparation of magnetic-HAp NCs by template assisted method, Mir and co-workers used nano templates of aqueous ferrofluids with different concentrations (20, 40, 60 and 80 μl) and stabilized them with polyvinyl alcohol. Polyvinyl alcohol ferrofluids were incorporated on the HAp matrix resulting in biologically active magnetic materials [59]. Singh et al. synthesized the magneto HAp nanotubes by using a template of composite of polycaprolactone-magnetite NPs. The surface activation was done in alkaline pH and deposition of apatite minerals occurs. According to the morphology, the outer surface was HAp shell with 137 nm thickness and 650 nm dimensions. The ferro-magnetic behaviour of the product was shown with 27.20 emug<sup>-1</sup> [60]. In another work, the HAp template was used to produce the NCs by CoFe<sub>2</sub>O<sub>4</sub> having a coating of SiO<sub>2</sub> with core-shell about 50 nm. The use of HAp template prevented the aggregation of nanosized magnetic particles. Moreover, pore size of structures was reported 10–20 nm with 212.8 m<sup>2</sup>g<sup>-1</sup> surface area. Additionally the magnetic composites were used in excellent drug delivery as presented in Fig. 8 [58]. Ali and coworkers synthesized magneto HAp NCs with a molecularly imprinted polymer using dibenzothioephene templates. The product had a surface area of 961 m<sup>2</sup>g<sup>-1</sup> and 0.398 cm<sup>3</sup>g<sup>-1</sup> pore volume. Additionally, thermodynamic and kinetic studies were accomplished [61]. Another work reported by Cui et al. involved a template of water-soluble magnetic nanoparticles of Fe<sub>3</sub>O<sub>4</sub> or MnFe<sub>3</sub>O<sub>4</sub> stabilized by Al(OH)<sub>3</sub> to synthesize fluorescent and magneto HAp nanoparticles. Furthermore, polymers of bisphosphonate polyethylene glycol were applied for the better colloidal stability in aqueous medium and 64Cu was incorporated effectively [62].

The modern template method has proven to be very suitable for the controlled synthesis of magnetic nanoparticles and especially in controlled drug delivery to targeted cell lines.

#### 2.6. Synergistic synthesis method

A synergistic method is the combination of two or more synthesis methodologies like mechanochemical-hydro/solvothermal, and microemulsion-hydro/solvothermal. A synergistic method is used to improve the properties, morphology and the crystalline nature of the nanomaterials. Mondal et al. used a synergistic method (solvothermal-chemical precipitation) for the preparation of magnetic HAp nanoparticles in which iron oxide was coated with HAp. These coated particles presented 40.6 emug<sup>-1</sup> magnetic saturation under 1.5 T magnetic field and 300 K temperature [63]. Xu and co-workers synthesized Pt

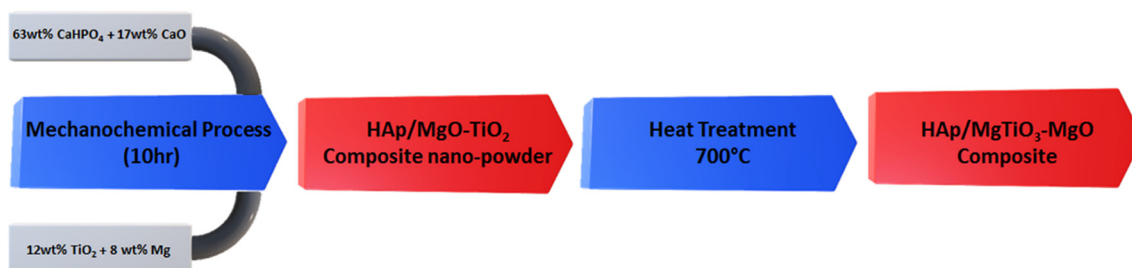


Fig. 5. Graphical representation of the formation of HAp-magnesium titanate nanocomposite by mechanochemical process and subsequent thermal treatment. Regenerated with the permission of [48]. Copyright (2013) Springer Nature.

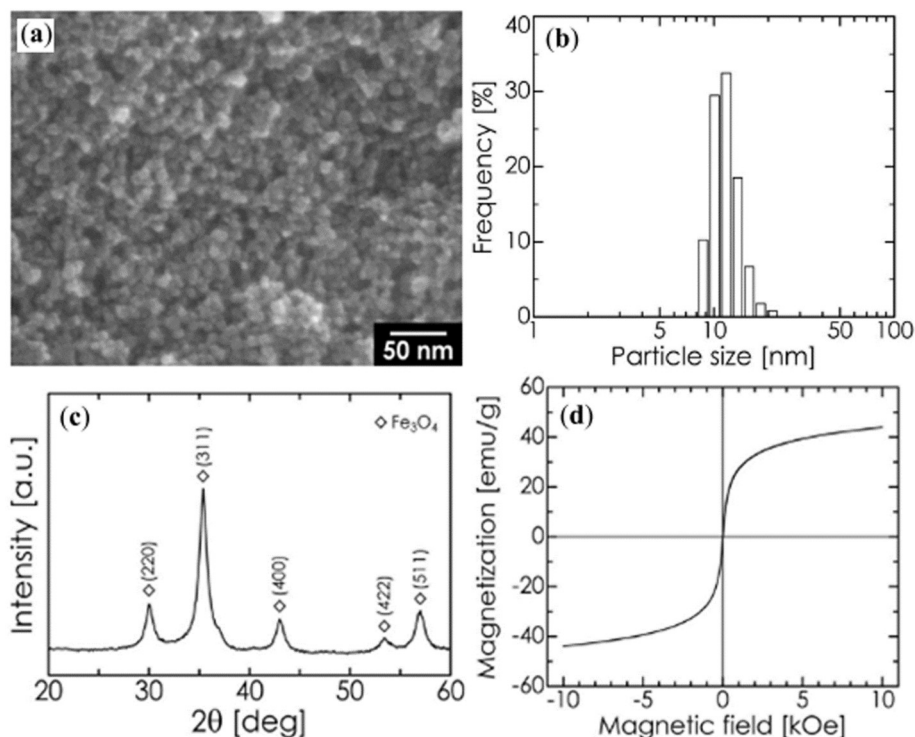


Fig. 6. (a) SEM image, (b) distribution of particle sizes, (c) XRD pattern and (d) magnetization-magnetic field hysteresis loop of  $\text{Fe}_3\text{O}_4$  NPs [51].

loaded HAp NCs with sodium citrate, sodium dodecyl sulphate and hexamethylenetetramine by hydrothermal-chemical reduction processes. These catalytic magnetic HAp materials were used for the absorbance of oxygen active molecules such as HCHO [64]. Gu and companions reported a green method for the preparation of  $\text{Fe}_3\text{O}_4/\text{HAp}$  mesoporous NCs by the combination of chemical precipitation-hydrothermal and resulted in 100–150 nm length and 20 nm width mesoporous NCs with 2.0 nm pore size having superparamagnetic behaviour with  $16.20 \text{ emu g}^{-1}$  [65]. Yao Zhao et al. synthesized chitosan/collagen/ $\text{Fe}_3\text{O}_4/\text{nHAp}$  organic-inorganic combinations of magnetic scaffold. These composites were reported to be biologically active having good biocompatibility *in vitro* and *in vivo* with significant potential for tissue and bone regeneration [66]. Abbasi et al. used a synergistic method with the assistance of spray drying techniques to make  $\text{Fe}_2\text{O}_3/\text{HAp}-\text{Ag}$  NCs. HAp core-shell was supported by Ag. These magnetically recyclable catalysts were utilized efficiently in the Pechmann condensation of phenols and  $\beta$ -ketoesters. This method was suitable to have a good yield, eco-friendly, being less time consuming with minimum work up procedure, and easy recovery from solution with the help of an external magnet [67].

From the above discussion about the synthesis methodology of magnetic HAp NCs, it is concluded that most reports presented non-homogeneous structures with biomedical properties, but a few reports showed highly crystalline, regular and good structures with enhanced biomedical properties. Moreover, in most of the cases there are rod shaped and core-shell magnetic HAp NCs offered better properties with remarkable results as compared to the rough and irregular particles.

### 3. Applications of magnetic HAp nanocomposites

Magnetic HAp NCs can be defined as a mixture of these two components embedded together to form a single system which delivers enhanced multifunctional properties because of hybridization nature. These versatile properties are strongly dependent on the size, structure

and concentration of the composites. For example, in magnetic HAp core-shell NCs, the core material is encapsulated by another outer shell material and they are expected to demonstrate multifunctional properties that change from the intrinsic properties of individual materials. These materials possess high surface area, good biocompatibility and strong mechanical strength. Because of the distinct surface functionalities and synergetic properties of magnetic HAp NCs, these NCs have obtained great interest in biological applications like drug delivery, tissue engineering/bone regeneration, environmental remediation (heavy metals & dyes removal), catalysis, antimicrobial, biosensors and fire resistance materials as shown in Fig. 9. The magnetic ability of these materials makes them useful in purification properties and biosensors and electrical conductivity help in the transmission of signals. Furthermore, they have promising features in targeted drug delivery because external electric and magnetic fields control the response of stimuli and drug can be delivered to the desired area. Magnetic HAp NCs are also utilized in multimodal imaging therapeutics and diagnosis of cancers [68].

In the following section, we will discuss the structure property relationship, surface functionalities and potential applications of magnetic HAp NCs in the biomedical field.

#### 3.1. Drug delivery

Significant progress has been made in controlled drug delivery system during the last seven decades. Oral and transdermal sustained release systems were established during the 1st generation (1950–1980) of drug delivery. In the 2nd generation (1980–2010), research was focused on the development of self-regulated drug delivery systems, and nanoparticle-based targeted delivery systems. In controlled and targeted drug delivery mechanism, drug carriers play a key role in the drug delivery system for the release and efficiency of the system [69,70]. A good drug carrier possesses easy attachment and easy release of the drug, large surface area for drug loading and biocompatibility [71]. Many researchers reported that magnetic HAp NCs have proved to be suitable for controlled drug



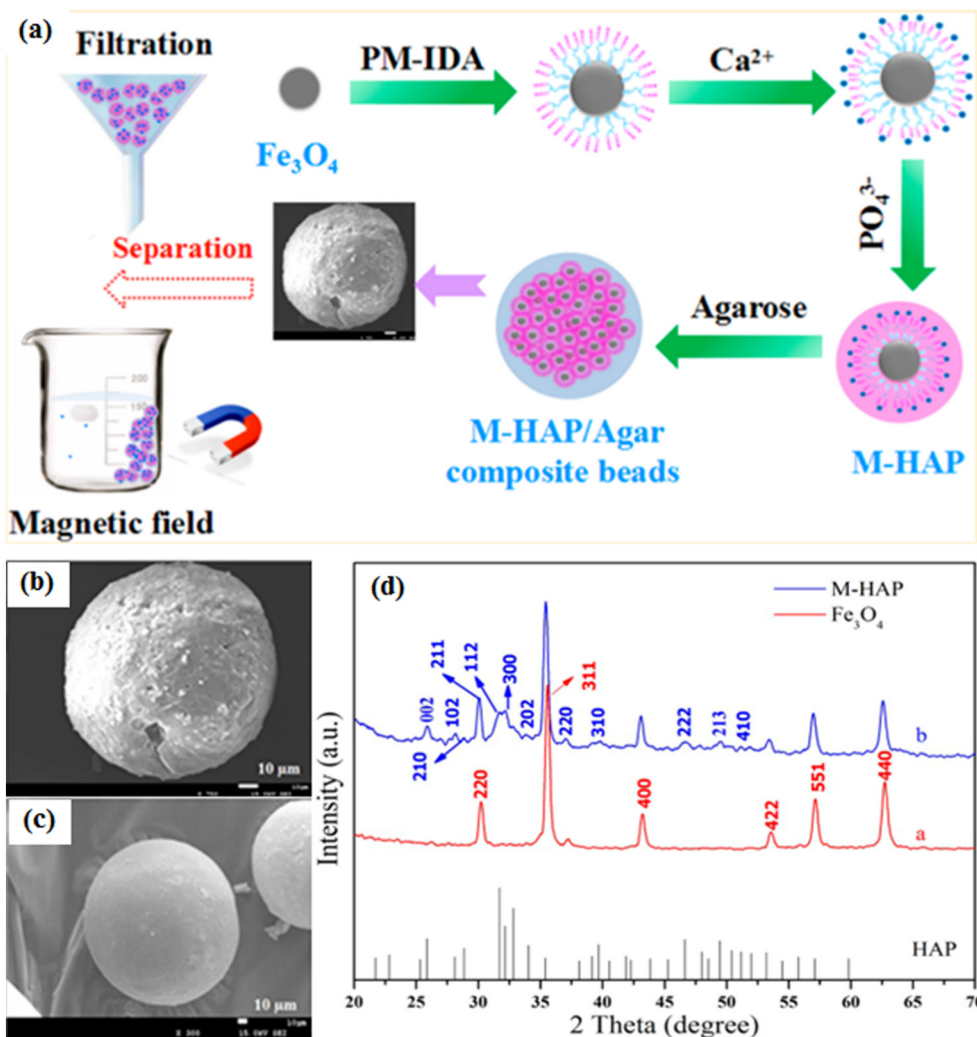


Fig. 7. (a) Graphical illustration of M-HAP/Agar composite beads synthesized by modification with PM-IDA, (b, c) SEM image of M-HAP/Agar and pure agarose beads respectively, and (d) XRD patterns of  $\text{Fe}_3\text{O}_4$  and M-HAP nanoparticles. Reprinted with permission of [53]. Copyright (2017) American Chemical Society.

delivery system. Because HAp retains an additional feature of high capacity of drug loading and unloading due to OH group in HAp and it can make hydrogen bond to OH containing drug and the magnetic part in composite helps to target the cell lines with the help of an external field. Furthermore, HAp coating protects the agglomeration of polymers, has high biocompatibility and offers stability with respect to temperature and pH. Drug loading and unloading can be calculated by following formulas;

$$\text{Drug entrapment efficiency} = \frac{\text{Drug initial} - \text{Drug in supernatant}}{\text{Drug initial} \times 100\%}$$

$$\text{Drug loading content} = \frac{\text{Drug initial} - \text{Drug in supernatant}}{\text{Amount of composite material} \times 100\%}$$

A study was reported to show the anti-tumor ability of lamellar magnetic HAp (LM-HAp) and lamellar HAp (L-HAp) with various concentrations targeting the MDA-MB-231 cell line of breast cancer in human. The results obtained from scratch and adhesion assays suggested that magnetic nanoparticles incorporated with HAp showed stronger capabilities to impair the migration and adhesion of MDA-MB-231 cells than L-HAp because the superparamagnetic nanoparticles have the ability to impair the endothelial progenitor cell (EPC) migration. These materials showed low cytotoxicity and efficiently decreased the adhesion and mobility of the cell. Results proved that magneto HAp

material showed greater inhibition on adhesion and mobility of cancer cells as compared to other material and was safe for gene vectors. Western blotting results proved the impact of magnetic HAp material on phosphorylation of integrin  $\beta 1$  [72].

Another study involved the targeted anticancer drug delivery by cobalt doped HAp NCs. The presence of a magnetic part ( $\text{Co}^{+2}$ ) showed some prominent features for HAp in attachment and release of the drug. Zeta potential examination showed that Co-HAp had a good ability for adsorption of protein due to positive surface potential by  $\text{Co}^{+2}$ . Furthermore,  $\text{Co}^{+2}$  enhanced the ability of HAp in the release of 5-Fluorouracil (an anticancer drug) and haemocompatibility. This sustained drug delivery was associated with the covalent bonding of  $\text{Co}^{+2}$  and HAp with the drug molecules. The results demonstrated the efficiency of Co-HAp NCs in drug delivery proposed to be effective for bone growth, wound healing and treatment of tumor cells due to its promising magnetic and drug loading/unloading characteristics [24]. Currently, mesoporous hollow structures attain potential interest because of high specific area for drug loading capacity. In this context, mesoporous magneto HAp hierarchical microspheres were reported with high drug-loading efficacy and pH responsive drug release ability. The designed structure showed high loading amount/efficiency of hydrophilic antibiotic vancomycin which is attributed to hollow and mesoporous structures, H-bond interactions between HAp and OH

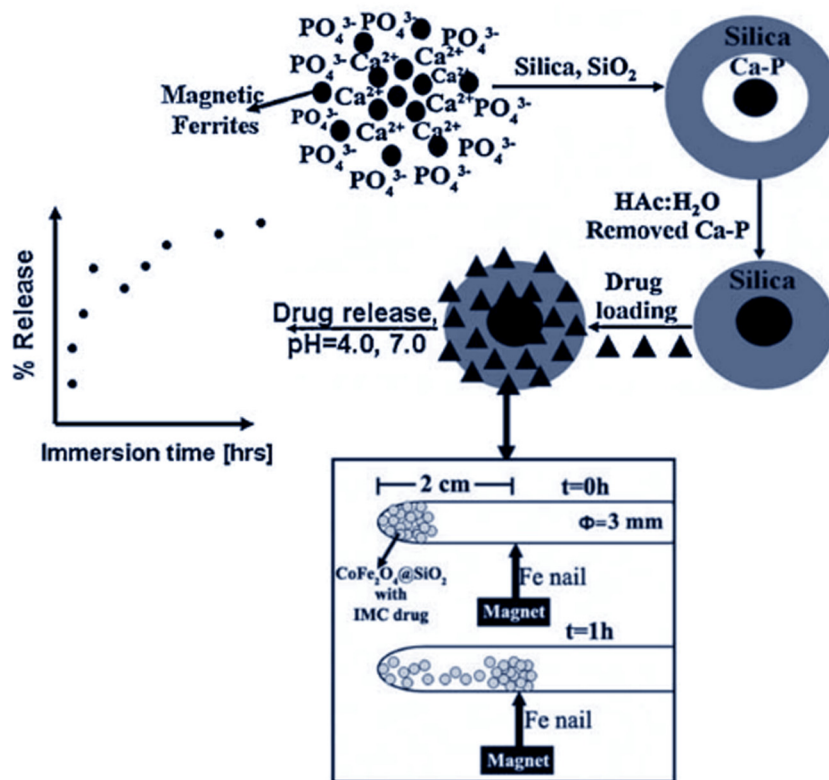


Fig. 8. Mechanism for the synthesis of CoFe<sub>2</sub>O<sub>4</sub>@HAP NPs coated by SiO<sub>2</sub> and pH controlled drug release process using external magnet. Reprinted with the permission of [58]. Copyright (2011) Elsevier B.V.

group of vancomycin. The sustained drug release phenomena were observed in the hollow magnetic HAp microspheres as compared the conventional HAp nanoparticles. This study revealed that Fe<sub>3</sub>O<sub>4</sub> slowed down the process of degradation of HAp and enhanced bone cell proliferation activity and the expression of multiple osteogenic genes, leading to the successful implementation in bone regeneration therapy [29]. In other research, ferrofluids HAp

NCs were prepared as drug delivery vehicles. Polyvinyl alcohol was used for the stabilization of ferrofluid templates. Vibrating sample magnetometry proved the superparamagnetic behaviour of the sample due to iron particles, and HAp provided biocompatibility and a porous surface for the drug attachment [59].

It is well known that the silica coating improves biocompatibility. Indomethacin (IMC) drug loaded on NCs of CoFe<sub>2</sub>O<sub>4</sub> with the coat of SiO<sub>2</sub> and template of Hap has been reported and the results showed that drug release was high at 4 pH relative to neutral pH. Furthermore upon aging about 50 h the concentration of magnetic iron and cobalt ions release was decreased [58]. Mesoporous Fe<sub>3</sub>O<sub>4</sub>/HAp NCs were also used for targeted chemotherapy of cancer using doxorubicin (DOX). DOX release was controlled by pH response and results showed that gradual decrease in pH value gave the slow and safe release of the drug (43% in 100 h). The presence of magnetic particles in DOX-loaded Fe<sub>3</sub>O<sub>4</sub>/HA nanocomposite are responsible for sustained drug release due to the low degradation of IONPs [65]. Work on targeted cancer drug delivery was carried out and iron oxide (IO) with HAp NCs were proven to be very efficient magnetic hyperthermia after incubated with osteosarcoma MG-63 cells (Fig. 10 a, b). The IO and IO-HAp NCs heated to 65 °C and 54 °C in 10 min, respectively, under an alternating magnetic field. The HAp coating onto the surface of IO acts as an insulator to decrease the temperature. However, this temperature (42–47 °C) is enough to kill the cancer cells without impacting normal cells.

The *in vitro* killing behaviour of osteosarcoma MG-63 cells lasted for 30 min as shown in Fig. 10 (c, d) [63].

Another study was reported regarding the biocompatibility of γ-Fe<sub>3</sub>O<sub>4</sub> in HAp nanoparticles and investigated for cancer therapy by magnetic hyperthermia. Cytotoxicity effects were checked by the exposure of the sample to sarcoma osteogenic (SAOS-2) human cell lines. The study showed that the magnetic-nano HAp matrix endorsed higher adhesion ability to SAOS-2 cells, when compared to individual materials, resulting in the treatment of osteosarcoma cells by magnetic

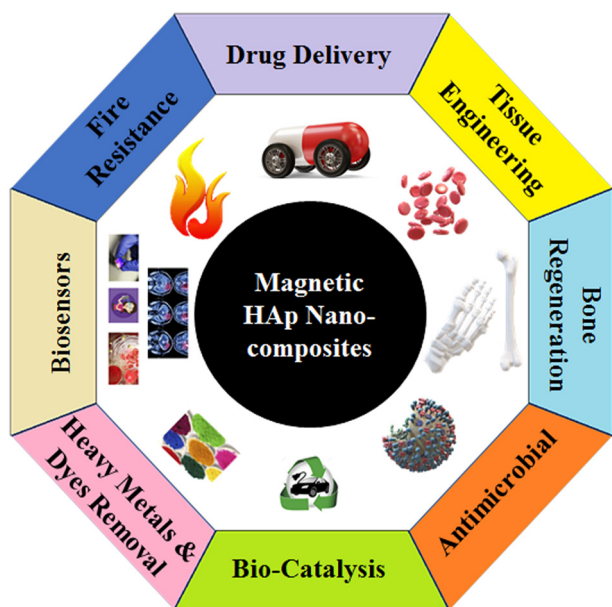
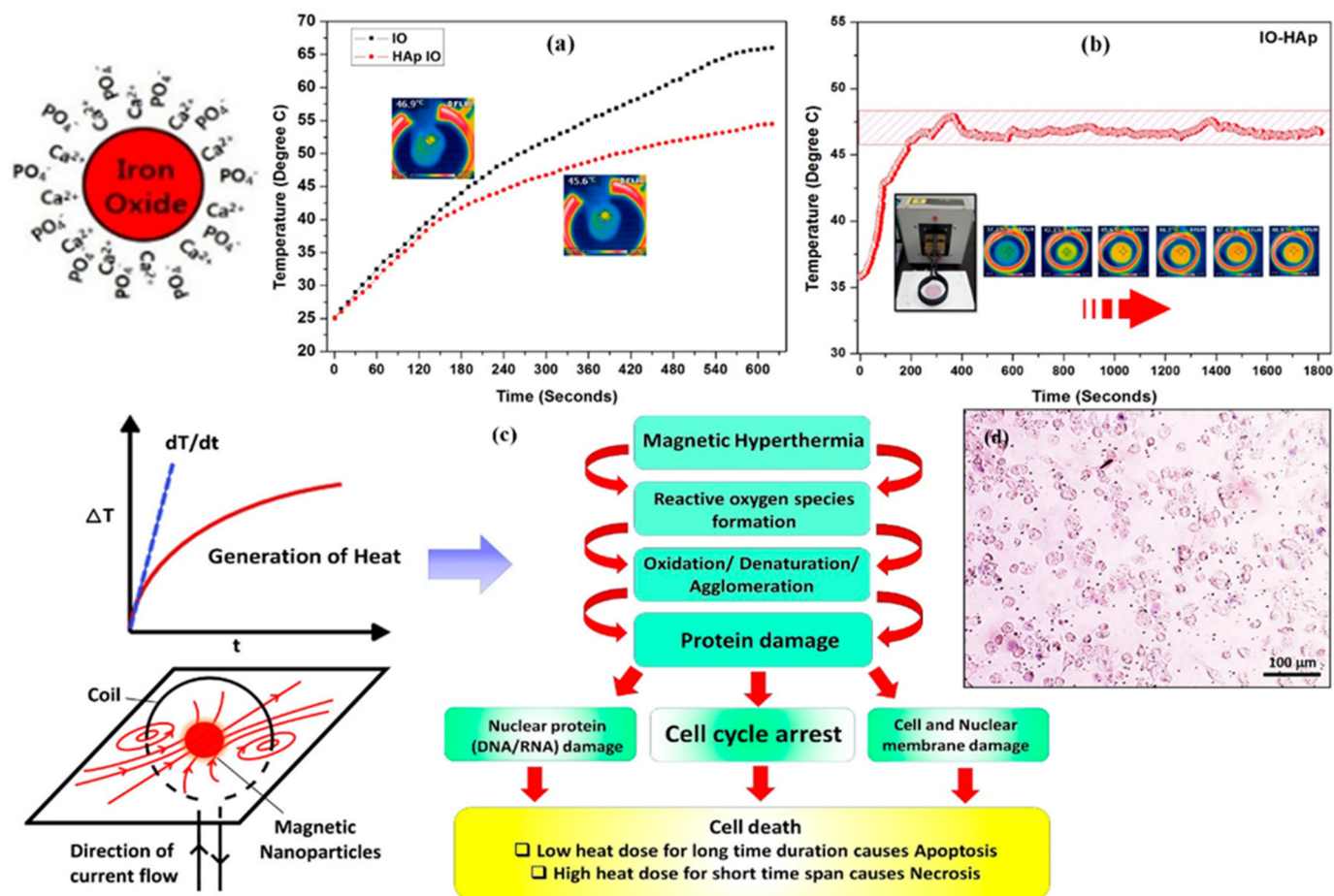


Fig. 9. A representation about the applications of magnetic HAp nanocomposites.



**Fig. 10.** Schematic illustration with Magnetic hyperthermia properties of (a) Iron oxide and HAp coated iron oxide (IO-HAp) (b) hyperthermia investigation of IO-HAp and their corresponding infrared thermal study (c) cell death process using magnetic hyperthermia (d) Iron oxide-HAp NCs with the cell for 24 h with a concentration of 100 µg/mL [63].

hyperthermia [34]. 3-Aminopropyl triethoxy silane (APTES) modified  $\text{Fe}_3\text{O}_4/\text{SiO}_2/\text{HAp}$  NCs were designed to investigate the drug release mechanism in the gastrointestinal tract. The surface area of APTES@ $\text{Fe}_3\text{O}_4/\text{SiO}_2/\text{HAp}$  is less than  $\text{Fe}_3\text{O}_4/\text{SiO}_2/\text{HAp}$ . However, the drug loading capacity of APTES@ $\text{Fe}_3\text{O}_4/\text{SiO}_2/\text{HAp}$  is better because of amino groups strongly attached to the OH of HAp. These composites showed significant drug release 100% and 15.6% behaviour in the gastrointestinal tract at pH 6.8 and pH 1.2 respectively and the aging time was 30 h [39].

One promising work for the treatment of lung cancer by Pt-Fe-HAp dual-functional chemo-hyperthermic NCs was presented by Ching-Li Tseng et al., in which anticancer behaviour and biocompatibility were checked against 3 T3 cells. The hyperthermia effect on adenocarcinoma cells (A549) of human lung was obtained by the test method of lactate dehydrogenase. Generally, HAp is good drug transporter as it is stable at neutral atmosphere but unstable at lower pH. Therefore, degradation of HAp easily takes place in endosomes because of low pH value and NPs ( $\text{Pt}^{2+}$ ) escape from the assembly to produce toxicity in the nucleus leading to cell death. Also, Pt-Fe-HAp NCs produce enough heat under the alternating magnetic field to kill the tumor cells. These NCs were extremely toxic to adenocarcinoma cells (A549) with no harm for fibroblast cells. It proved the efficiency of Pt-Fe-HAp dual functional chemo-hyperthermic NCs to treat lung cancer [73]. Targeted drug delivery behaviour of magnetic  $\text{Fe}_3\text{O}_4/\text{HAp}$  nanorod shaped composites was studied due to the excellent magnetic properties, mesoporous structure, and high surface area. Andrographolide drug was loaded on magnetic NCs and targeted the cancer cells (A431) of human skin epidermis. The magnetic part of the composites helped in the targeted delivery and release of the drug. Results were concluded by apoptosis and

antiproliferative activities and proved the biocompatibility and suitability of  $\text{Fe}_3\text{O}_4/\text{HAp}$  MNCs for targeted drug delivery applications [74].

These reports all enlighten the effectiveness, suitability and biocompatibility of magnetic HAp NCs for targeted drug delivery applications with sustained drug release to cancer cells under suitable and controlled conditions of pH, concentration, magnetic field and temperature.

### 3.2. Tissue engineering

The tissue engineering can deliver substitute tissue for medical use [75]. Various reports are available to show that magnetic HAp NCs are useful for tissue engineering as compared with HAp composites scaffolds [76]. This is because magnetic entities have the ability to control the position and drug release process by external magnetic field with active bioimaging. In addition, magnetic nanoparticles show the significant effect of osteoinduction to enhance the growth of tissues.

In this regard, superparamagnetic Fe-HAp NCs modified by polylactic acid were used for tissue engineering application reported by Michele Iafisco et al. These MNCs showed effective behaviour towards mesenchymal tissues and especially large amount of Fe-HAp (30 wt%) exhibited good cell proliferation results as compared to the lower amount (1 wt%). [55]. Other research was published regarding the suitability of Fe/Sr co-substituted HAp composites for tissue engineering. These composites were appropriated for a human mesenchymal cell having high compatibility with blood and magnetic particles enhanced the drug release capability and rate tissue repair profile of the magnetic HAp NCs [33]. MNCs of poly(1-caprolactone)/iron doped HAp (PCL/FeHAp) were used for tissue engineering. The inclusion of

Fe-HAp gave good mechanical characterization, improved substrate hydrophobicity and showed superparamagnetic behaviour lowering the coercive field. Furthermore, magnetization was proportional to the temperature sweeps. Biological effectiveness against mesenchymal cells was approved by AlamarBlue test and LSM (laser scanning microscopy). *In vitro* cell adhesion study was carried out by using human mesenchymal stem cells (hMSCs) and results predicted the good spread and excellent adherence of hMSCs on PCL/FeHAp as compared to the PCL [77]. A study was reported about the development of Fe<sup>+2</sup>/Fe<sup>+3</sup>-HAp fused biomimetic frameworks and investigated their influence on osteoblast-like cells. Results showed that magnetic HAp NCs possessed superparamagnetic nature and super-paramagnetic scaffolds were more suitable for cell proliferation as compared to non-magnetic scaffolds. Iron induced superparamagnetic behaviour under an external static magnetic field improved the cell adhesion and proliferation process. [78]. One previous work was about tissue engineering using iron-HAp MNCs *via* marrow of rat. Magnetic nanoparticles showed excellent DNA affinity and a considerable increase in transverse section in mesenchymal cells having the gene of glial cell line-derived neurotrophic factor (GDNF) as compared to non-magnetic nanoparticles [79].

In the field of tissue engineering, magnetic HAp NCs showed appealing possibilities due to their unique physio-chemical features that enhance their range of applications. The above discussion testifies that MNCs are promising in cell proliferation, cell adhesion, and faster differentiation of osteoblast cells for tissue engineering as compared to non-magnetic composites.

### 3.3. Bone regeneration

Bone regeneration is a hot topic of research for the modern era. Scientists have been working in this field by using various organic, inorganic and composite nanomaterials [80–84]. However, MHAp NCs are taking considerable intentions owing to their special physical and chemical features, magnetic behaviour and biocompatibility. Bone regeneration using magnetic HAp coating with magnetic bio-glass (CaO-SiO<sub>2</sub>-P<sub>2</sub>O<sub>5</sub>-Fe<sub>3</sub>O<sub>4</sub>) has been reported. The presence of Fe<sub>3</sub>O<sub>4</sub> enhanced the perpendicular growth of HAp nanorods and HAp particles changed into bulky particles in the absence of Fe<sub>3</sub>O<sub>4</sub>. Additionally, bone marrow cells were used to examine biological feasibility and fitness and resulted in healthier adhesion of cell, proliferation and spreading for MHAp (HA) coatings as compared to other composites. These excellent results recommended magnetic HAp NCs as potential candidate for bone implants [26]. MHA mesoporous NCs were also utilized for the treatment of bone disorders. Cell tests were performed *in vitro* on stromal cells of human bone marrow and it showed the efficiency of magnetic HAp NCs by cell proliferation, cell adhesion and the stimulation of osteogenic differentiation. Similarly, as discussed above, Fe<sub>3</sub>O<sub>4</sub> NPs inside the mesoporous structure revealed a positive influence on the human bone marrow stromal cells by stimulating adhesion, proliferation and the osteogenic differentiation. The results indicated the potential of magnetic HAp NCs for the cure of complex bone ailments [21]. Iron-doped HAp NCs for the applications in the field of bone tissue regeneration was reported and the *in vitro* study was carried out on the human osteoblast cells Saos-2 for the time period of 1, 3 and 7 days in the presence and absence of 320 mT magnetic field and the results were compared with the commercially available HAp particles. Osteoblast cell proliferation activities were significantly increased in the presence of a magnetic field as compared to no magnetic field and HAp material. This study supported the efficiency and biocompatibility of Fe-HAp NCs for bone regeneration, and also may have future platform for molecular imaging for diagnosis and therapeutic applications [85]. In a recent work, Fe/Sr co-doped HAp NCs reported as a bone substitute. The study proved the effectiveness of magnetic nanocomposite in osteogenic differentiation and osteoblast proliferation. Fe/Sr doping in HAp possessed synergetic effects and improved the deposition of calcium, ALP activity, and RUNX2 expression. The results of osteocalcin and osteopontin proteins for

MC3T3-E1 cells proved the suitability and biocompatibility of Fe/Sr co-doped HAp NCs as a substitute of bone [32]. A study was reported about the effectiveness of chitosan/collagen/Fe<sub>3</sub>O<sub>4</sub>/nHAp (CS/Col/Fe<sub>3</sub>O<sub>4</sub>/nHAp) magnetic scaffolds in bone regeneration. The *in vitro* study showed higher cell adhesion, proliferation and osteogenic distinction. Excellent bioactivity and *in situ* biomimetic mineralization was verified by mineralization tests. Furthermore, *in vivo* skull defect model of rat, the magnetic composites provided an improved bone regeneration effect then the control (CS/Col/nHAp) as presented in Fig. 11 [66]. In a related work, firstly HAp/chitosan with hexagonal magnetic SrFe<sub>12</sub>O<sub>19</sub> was merged to the bone scaffolds to combine with endogenous stem cells. After this, lanthanum was incorporated for immune response of host cells. This magnetic lanthanum doped HAp/chitosan (MLHAp/CS) composites demonstrated good biocompatibility and enhanced the osteogenic differentiation of rat bone marrow mesenchymal stem cells for bone repair applications [35].

The advances of magnetic HAp NCs in the field of bone regeneration are justified from above discussion. The results of this work enable us to understand that magnetic HAp NCs presents promising scaffolds for bone regeneration, bone substitution and detection of defects in bones by accelerating the cellular proliferation and adhesion properties

### 3.4. Antimicrobial agent

The inhibition or assassination of disease-causing microbes (fungus, bacteria and viruses) is associated with antimicrobial activity [86]. Hydroxyapatite by nature possesses limited antimicrobial behaviour, so to enhance its antimicrobial activity, researchers performed doping of magnetic ions into HAp to design hybrid nanoparticles [87,88]. Many pieces of research showed the efficient antimicrobial behaviour of magnetic HAp NCs.

Work was carried out on the synthesis of multifunctional Sr/Fe co-doped HAp NCs and their comparative antimicrobial behaviour was assessed against two bacterial strains of *Staphylococcus aureus* (Gram positive) and *Escherichia coli* (Gram negative) with variable concentrations as of NCs presented in Fig. 12. The results demonstrated excellent behaviour of all the samples against *S. aureus* with high zone of inhibition (Fig. 12 (a-f) *S. aureus*) as compared to the *E. coli* (Fig. 12 (a-f) *E. coli*). Further, the NCs with maximum concentration of Fe showed remarkable results in comparison to the pure HAp (Fig. 12 g) [32]. In another study, Fe<sub>3</sub>O<sub>4</sub>-HAp NCs were used against *Micrococcus luteus* (Gram-positive) and *Escherichia coli* (Gram-negative) bacterial strains. Gram-negative bacteria were affected suddenly, and after 2 h of incubation there was a rapid decline in the viability of cells. According to Gram-positive bacteria, hour there was the resistance by cells up to 4th then rapid effect noted in 5th hour. Results concluded that *Escherichia coli* surrendered earlier as compared to *Micrococcus luteus* in the presence of magnetic HAp NCs [22]. Amir Seyfoori et al. prepared ZnFe<sub>2</sub>O<sub>4</sub>/HAp NCs and were used as an antibacterial agent against *Staphylococcus aureus* resulted in a positive effect even at concentration. An excellent inhibitory outcome was shown at 0.078 mg/L optimal dose. Ultra-small iron nanoparticles can easily enter into the bacteria cells and stimulate the bacterial proliferation [89]. In another reported work Fe-HAp nanoparticle within polylactic acid were prepared and antibacterial analysis was performed against *Bacillus thuringiensis* and *Pseudomonas aeruginosa* bacterial strains. These iron-doped HAp NCs showed excellent results against both bacterial strains using the disc diffusion method. The results of MNCs were prominent as pure polylactic acid [90].

From this literature, it is obvious that magnetic HAp NCs possess excellent antimicrobial activity as compared to pure HAp. The efficiency depends upon the type of magnetic particle and concentration of composites.

### 3.5. Bio-catalysis

In modern research, biocatalysts have a role in the manufacturing of pharmaceutical products. There are many materials that act as a

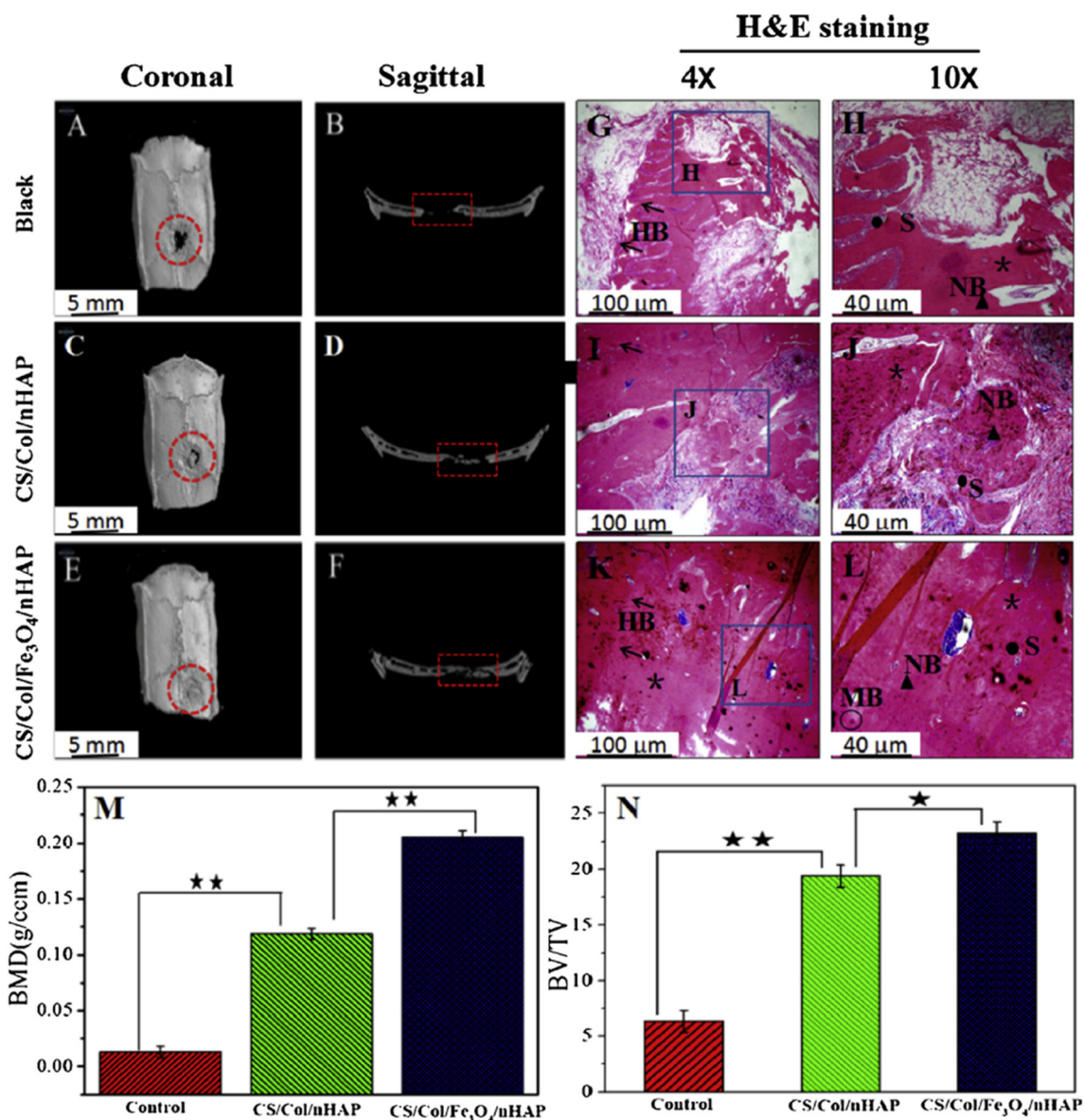


**Fig. 11.** (A–F) CT imaging, (G–L) histological assessment profile of rat calvarial defect regions before and after implanted after 12 weeks, (H,J,L) high magnification images of the framed area, (M) local bone mineral density study and (N) morphometric examination, bone volume/tissue volume, of new bone development for three groups in the defect site. \* $P < 0.05$ , \*\* $P < 0.01$ . Reprinted with the permission of [66]. Copyright (2018) Elsevier B.V.

promoter for the enzymes or boost the activity of a catalyst [91]. Magnetic HAp NCs are also playing an important role in the field of biocatalysis. In a study,  $\gamma\text{Fe}_2\text{O}_3$ -HAp NCs were utilized as a bio-catalysis. Lipase was tied to magnetic materials by covalent linkage without damaging the structure. A magnetic response was shown by restrained lipase while soybean oil inter-esterification. Results presented the predictable change in positional differences of triacylglycerols and fatty acids after enzymatic action [92]. Other work was reported in which metal ions ( $\text{Cu}^{2+}$ ,  $\text{Ni}^{2+}$ ) modified HAp was used for the immobilization of xylanase enzyme in bio-catalysis. The immobilization of xylanase made it reusable several times. The results represented that xylanase had a good affinity for HAp- $\text{Cu}^{2+}$  as compared to HAp- $\text{Ni}^{2+}$ . Furthermore, HAp- $\text{Cu}^{2+}$  gave 80% recovery of xylanase even in second cycle [93]. Takeshi Yabutsuka et al. synthesized  $\gamma\text{Fe}_2\text{O}_3$  coated by Apatite Nucleus assembly and then covered by simulated body fluid containing various elements including  $\text{Ca}^{2+}$  and  $\text{HPO}_4^{2-}$ . The magnetic apatite microcapsules were immobilized using urease. The prepared magnetic assembly coated by bone like apatite revealed urea decomposition ability

in water and appropriate for enzyme immobilization [94]. An interesting research was reported for the recovery of lipase enzyme by using magnetic  $\text{CoFe}_2\text{O}_4$ /HAp NCs (Fig. 13). The general scheme for enzyme immobilization is presented in (Fig. 13 a). Additionally, the effect of solvent on trans-esterification (1 h, 35 °C) was also studied as shown in (Fig. 13 b, c). The capability of enzyme recovery depended upon the  $\text{CoFe}_2\text{O}_4$  core. These bio-NCs proved to be very effective for trans-esterification of (R, S)-1-phenyl ethanol enantiomeric racemic mixture and converted into (R)-1-phenyl ethanol completely (Fig. 13 d, e). The magnetic part of composites supported the easy recovery of the enzyme by applying the magnetic field externally (Fig. 13 f). Results represented several cycle stability and utility of lipase by using magnetic HAp NCs [95].

In another work,  $\text{Fe}_3\text{O}_4$ /HAp MNCs were formed and modified by  $\beta$ -cyclodextrin grafted on the surface and used for the immobilization of lipase during ethyl valerate synthesis. These results confirmed that lipase on magnetic composites was stable, reusable and had the potential for synthesis in the organic phase [96]. A green and efficient catalyst was synthesized by magnetic HAp with propyl-sulfamic acid and  $\gamma\text{-Fe}_2\text{O}_3$ -

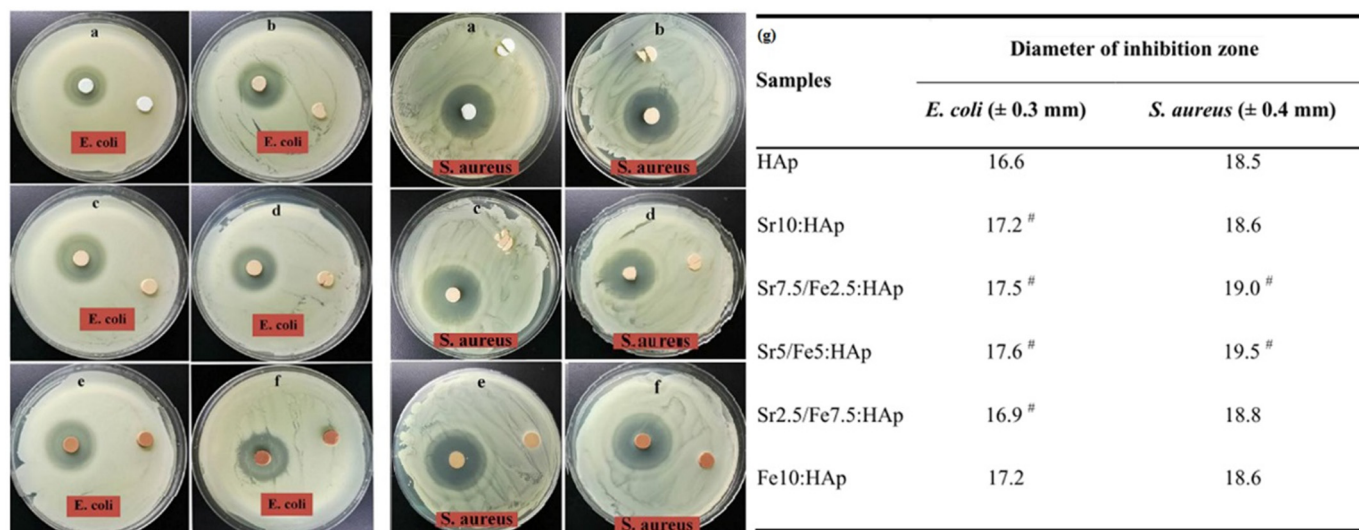


**Fig. 12.** The antibacterial properties of the AMX impregnated with various HAP bionanomaterials: (a) pure HAp; (b) Sr10:HAp; (c) Sr7.5/Fe2.5:HAp; (d) Sr5/Fe5:HAp; (e) Sr2.5/Fe7.5:HAp; (f) Fe10:HAp; (g) zone of inhibition measurement of. Reprinted with the permission of [32]. Copyright (2020) Elsevier B.V.

HAp-(CH<sub>2</sub>)<sub>3</sub>-NH<sub>2</sub>SO<sub>3</sub>H was reported to be the excellent green catalyst with at least ten times reusability. Furthermore, it was recoverable by applying an external magnetic field [97].

Such works prove the efficiency of magnetic HAp NCs in the modern field of bio-catalysis. These are environment friendly, reusable, cost-effective, competent and magnetically controlled composites for bio-catalysis.

### 3.6. Heavy metals & dyes removal

Industrial wastewater contains toxic contaminating reagents including inorganic and organic materials such as heavy metals and dyes and produce serious health effects on ecology. These poisonous pollutants are generated from textile and paint industries. Recently, various treatment procedures such as precipitation, ion exchange, ultrafiltration and phytoextraction have been employed to eliminate these dyes and heavy metals from the waste. However, these methods are expensive, consume high energy, and cause secondary and tertiary pollutants. Therefore, it is required to find cheap, efficient and eco-friendly method for the removal of heavy metals and toxic dyes [98]. Some researchers reported about the efficient and eco-friendly use of magnetic HAp NCs for the removal of heavy metals as well as toxic dyes. HAp/Fe<sub>3</sub>O<sub>4</sub> magnetic microspheres were used efficiently for the removal of Pb(II) from aqueous solution. The ion exchange method was used for sorption of Pb<sup>2+</sup> on magnetic composites at 3.0–6.0 pH value and for the removal of Pb<sup>2+</sup> from magnetic composites was done at 3.0–2.0 pH by the precipitation-dissolution method. The separation mechanism of heavy metal ions from HAp/Fe<sub>3</sub>O<sub>4</sub> magnetic microspheres was easy and convenient [23].

Industrial dyes are also agents of environmental pollution especially water pollution, so there is the need for removal of dyes along with heavy metals. Various reports have been showing the magnetic HAp NCs for toxic dyes removal. Removal of Congo red, Reactive orange 16 and Reactive orange 5 dyes from aqueous solution was reported by using NCs based on magnetic zeolite-HAp. The maximum adsorption of dyes was shown after 30 min at 2.0 pH with a concentration of dyes 80 ppm. These results showed adsorption capacities, 104.05 mg/g for Congo red, 88.31 mg/g for Reactive orange 16 and 92.45 mg/g for Reactive orange 5. Furthermore, the thermodynamic study proved the maximum adsorption at 40 °C. The magnetic zeolite/HAp NCs was efficient for the removal of these cationic dyes [100]. In another study, the magnetic HAp nano-powder (Sr<sub>5x</sub>Ba<sub>3x</sub>(PO<sub>4</sub>)<sub>3</sub>(OH)/Fe<sub>3</sub>O<sub>4</sub>) was used to

remove Congo red (anionic dye) and Malachite green (cationic dye) from their solution in water. The highest adsorption capacities were 526 mg/g for Malachite green and 417 mg/g for Congo red. Finally, magnetic HAp nano-powder was regenerated easily by an external magnetic field and it was useful up to five cycles [101]. Magnetic HAp-immobilized oxides multiwalled carbon nanotubes were used for water treatment and removal of Methylene blue dye and Pb(II) ions (Fig. 14). The adsorption capacities were reported 328.4 mg/g and 698.4 mg/g for Methylene blue and Pb(II) respectively and the comparative study proved an excellent performance of magnetic HAp NCs as compared to the pure components. Furthermore, the magnetic ability of composites facilitated the liquid-solid separation [99].

Removal of Cr(VI) from groundwater using magnetic HAp alginate beads was reported and these Fe<sub>3</sub>O<sub>4</sub>@n-HApAlg beads were reusable about five times with great efficiency by using NaOH as eluent. The magnetic NCs improved the sorption capacity of Cr(VI) up to 29.14 g/g as compared to separate components [31]. Fe<sub>3</sub>O<sub>4</sub>-SiO<sub>2</sub>-SrHAp microspheres were also used as an efficient sorption of Pb(II) acidic solutions in water with the highest immobilization of 345 mg/g at 3.0 pH (Fig. 15). The advantage of MNCs was to separate loaded Pb(II) easily with the help of a permanent magnet [102]. The removal of Pb<sup>2+</sup>, Cu<sup>2+</sup> and Co<sup>2+</sup> from wastewater was carried out by using phosphonemethyl iminodiacetic acid modified Fe<sub>3</sub>O<sub>4</sub>-HAp/Agar composite and adsorption capacity of magnetic composites was increased by the large size of beads. Results showed promising sorption as 842.6, 105.1, and 71.6 mg/g for Pb<sup>2+</sup>, Co<sup>2+</sup>, and Cu<sup>2+</sup> respectively. Due to the superparamagnetic behaviour and large size of Fe<sub>3</sub>O<sub>4</sub>-HAp/Agar composite beads, the recovery from the solution became easy [53]. HAp/Fe<sub>3</sub>O<sub>4</sub> NCs and simple HAp were used for the removal of lead ions from solution in water by applying an external magnetic field [36].

In a report about wastewater treatment, nanostructures of magnetic  $\gamma$ -Fe<sub>2</sub>O<sub>3</sub>/Fe-doped hydroxyapatite (HAp) were used for the removal of Cd(II). The determined adsorption was 258 mg/g at equilibrium, and it was much higher than pure HAp [38]. Heavy metal ions such as Zn(II) can also be removed from an aqueous mixture using core-shell of CoFe<sub>2</sub>O<sub>4</sub>-HAp NCs [103]. The magnetic HAp-chitosan/Fe<sub>3</sub>O<sub>4</sub> NCs presented remarkable results about 95% removal of AY220 and the degradation of AY220 was also higher than the pure components. Moreover, magnetic composites gave significant adsorption of Co<sup>2+</sup> released by the degradation of AY220 and after 5 cycles of reusable magnetic composites, the degradation reached 25.1% - 45.6% [104]. Various literatures reported about the removal of Methylene blue by using magnetic

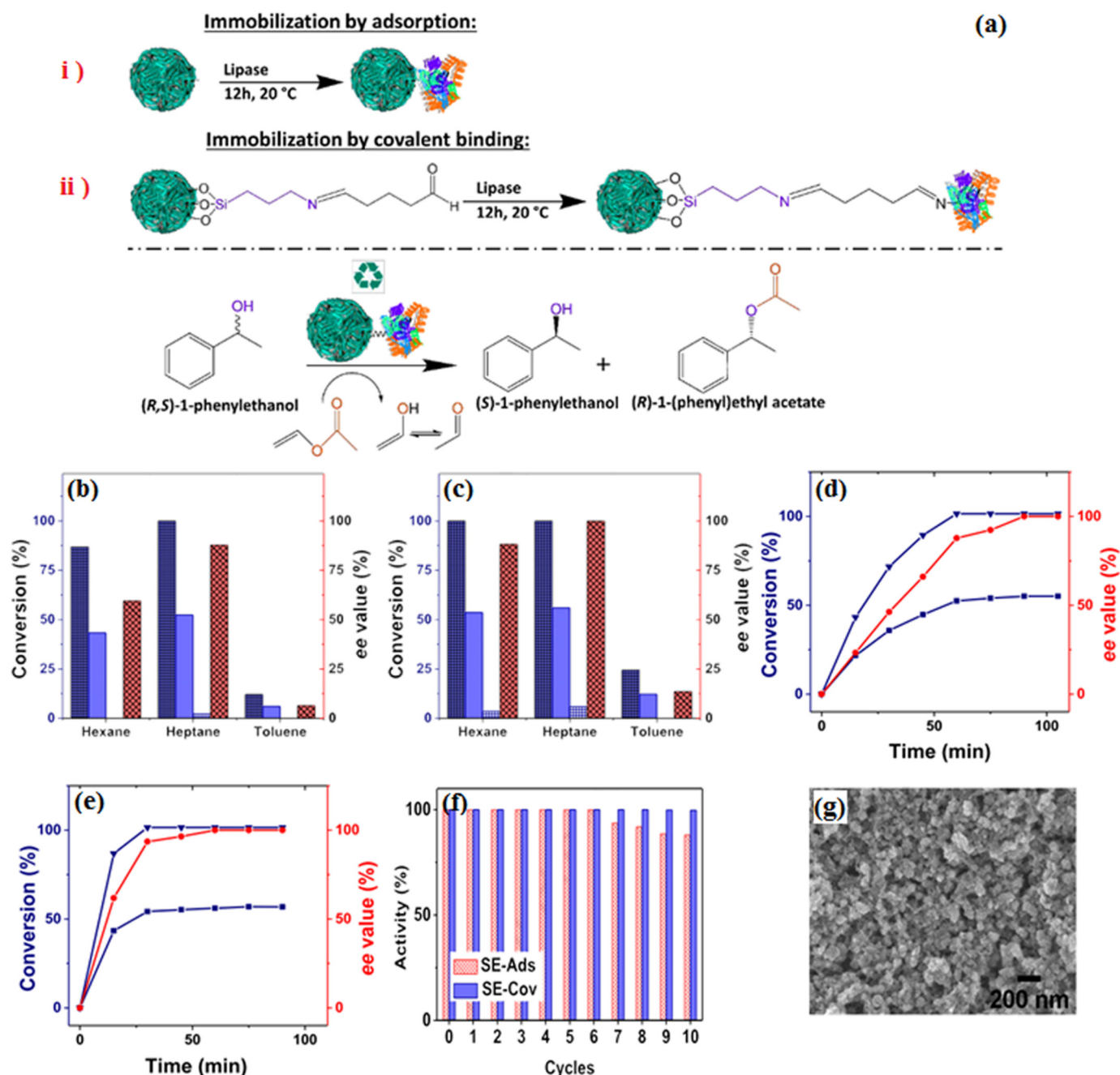


**Fig. 13.** (a) i) Enzyme immobilization showing time and temperature of reaction; ii) Enantioselective transesterification reaction of (*R,S*)-1-phenylethanol catalyzed by the bio-nanocomposite CoFe<sub>2</sub>O<sub>4</sub>/HAp/Lipase and CoFe<sub>2</sub>O<sub>4</sub>/HAp-APTES-Lipase. (b) Effect of solvent on Lipase adsorbed to CoFe<sub>2</sub>O<sub>4</sub>/HAp; (c) effect of solvent on Lipase covalently bonded to CoFe<sub>2</sub>O<sub>4</sub>/HAp-APTES. Conversion of (*R,S*)-1-phenylethanol: (d) Lipase adsorbed to CoFe<sub>2</sub>O<sub>4</sub>/HAp; (e) Lipase covalently bonded to CoFe<sub>2</sub>O<sub>4</sub>/HAp-APTES. (f) Enzyme activity on the transesterification of (*R,S*)-1-phenylethanol in heptane at 35 °C after several cycles of catalyst recovery and reuse. (g) SEM image of CoFe<sub>2</sub>O<sub>4</sub>/HAp core-shell nanocomposite. Reprinted with the permission of [95]. Copyright (2020) Elsevier B.V.

HAp NCs. The high adsorption performance due to the presence of magnetic oxides as compared to pure HAp [105–107].

These reported works demonstrate excellent sorption ability of magnetic HAp NCs for the removal of heavy metal ions as well as toxic dyes. An additional feature is the reusability of magnetic composites even after several cycles with remarkable efficiency.

### 3.7. Biosensors & molecular imaging

In the modern era of biomedical science, there are some challenging issues for accurate detection and measurements of microbes in biological samples, protein biomarkers and cell analysis. Many methods have been

developed for biomolecule measurements with high sensitivity for diagnostics. Magnetic nanoparticles are used in molecular imaging, biosensors and magnetic separations [108,109]. Magnetic HAp NCs are reported to be suitable for biosensors, MRI (magnetic resonance imaging), molecular and cellular imaging [110].

In this context, Gd doped Sr-HAp mesoporous rods were used for targeted MRI. These NCs showed good paramagnetic behaviour and auto fluorescence in blue. Furthermore, due to the magnetic nature, the composites showed controlled targeting against MCF-7 cell line. Results proved the effectiveness of magnetic HAp NCs in controlled targeted delivery with autofluorescence and MR-imaging [111]. In other research, carbon paste electrodes modified by NCs of  $\gamma$ -Fe<sub>2</sub>O<sub>3</sub>@

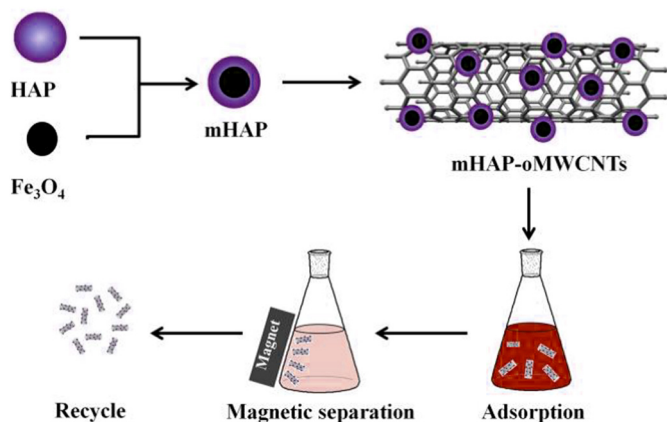


Fig. 14. Schematic description of heavy metal/dyes removal by using magnetic HAP NCs. Reprinted with the permission of [99]. Copyright (2017) Elsevier Inc.

hydroxyapatite/Cu(II) was applied as an electrochemical sensor for metformin. The outcomes of this research represented the effective increase in electrochemical recognition of metformin oxidation using magnetic HAP NCs. This sensor showed remarkable results in detection, quantification of metformin and was also useful for direct tests of urine and pharmaceutical samples [112]. Luminescence magnetic composites

are favorable in multifunctional applications such as optical/magnetic resonance imaging, biosensing and targeted drug delivery [113].

In another study, glassy carbon electrodes were modified by  $\text{Fe}_3\text{O}_4$ -HAP-molecularly imprinted poly-pyrrole and used as the photochemical biosensor for bilirubin. The sensitivity of this biosensor was high towards solutions of bilirubin with notable selectivity and the linear range was 0.1–17  $\mu\text{M}$  with 0.007  $\mu\text{M}$  detection limit. [114]. Detection of L-tyrosine is also possible by using biosensor of Fe-HAP and tyrosinase NCs with glassy carbon electrode modification. The amperometry and cyclic voltammery were followed for the L-tyrosine detection. At pH 7.0, the linear range was  $1.0 \times 10^{-7}$ – $10^{-5}$  M with 245 nM detection limit. The results showed the reproducibility, selectivity, stability with no interference while determining the L-tyrosine using the fabricated magnetic Fe-HAP biosensor [115]. In other reported work, Tb-HAP magnetic luminescent nanoparticles were prepared and a cellular study was carried out. These luminescent NCs were observable at 488 nm. Furthermore, the luminescent NCs were observed in mesenchymal cells of bone marrow in the rabbit by using a fluorescent microscope [116].

A study involving the promising behaviour of  $\text{Gd}^{3+}$  and indocyanine green doped HAP for molecular imaging was reported. Adsorption of X-rays and paramagnetic ability of doped NCs make them suitable for near-infrared, magnetic resonance and X-ray imaging. An *in vitro* study of doped HAP on human lymphocytes showed no harmful effect which proved the biocompatibility and multimode imaging agents [117]. Another work involved the multimodal imaging by using  $\text{Eu}^{3+}$ - $\text{Gd}^{3+}$  co-doped HAP NCs. The magnetization was increased by  $\text{Gd}^{3+}$

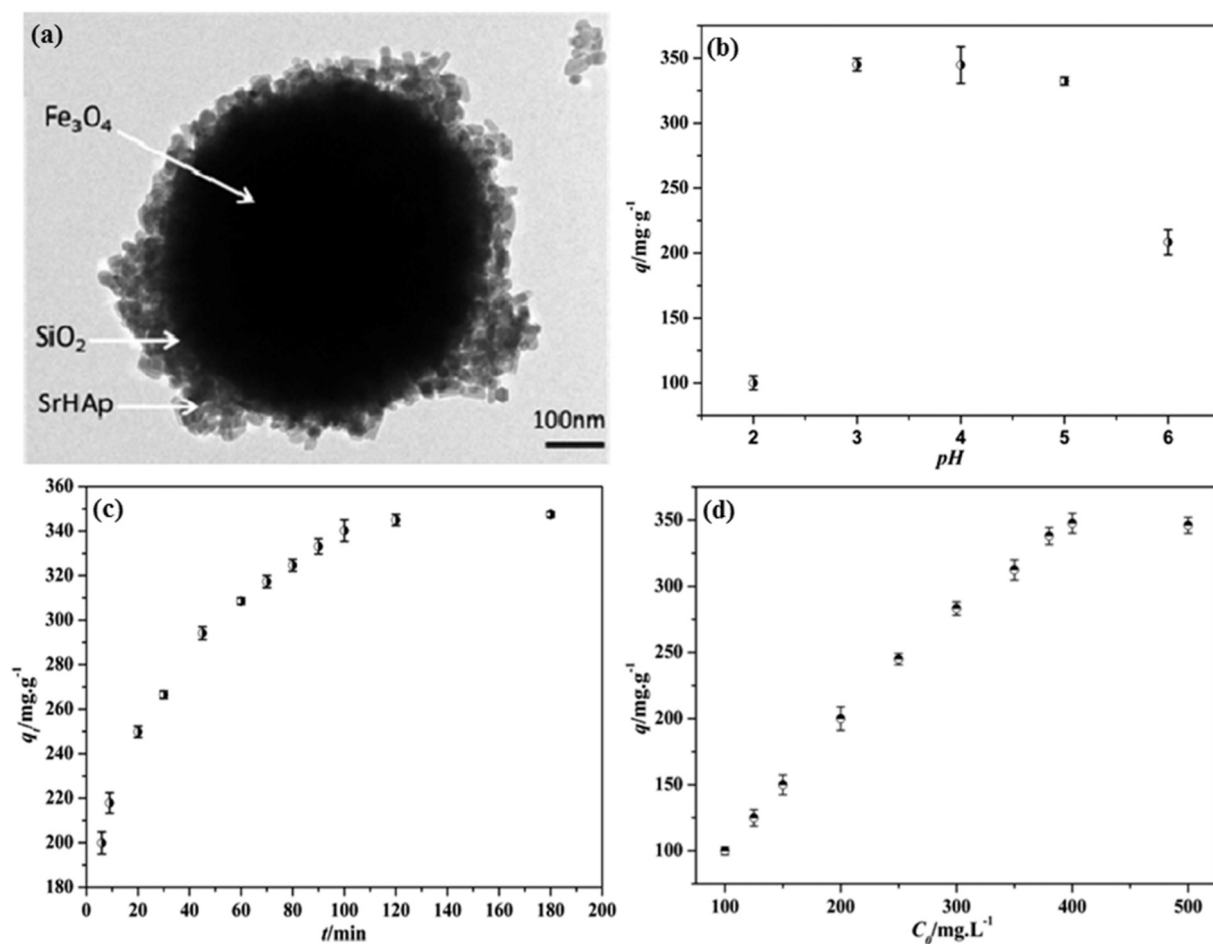
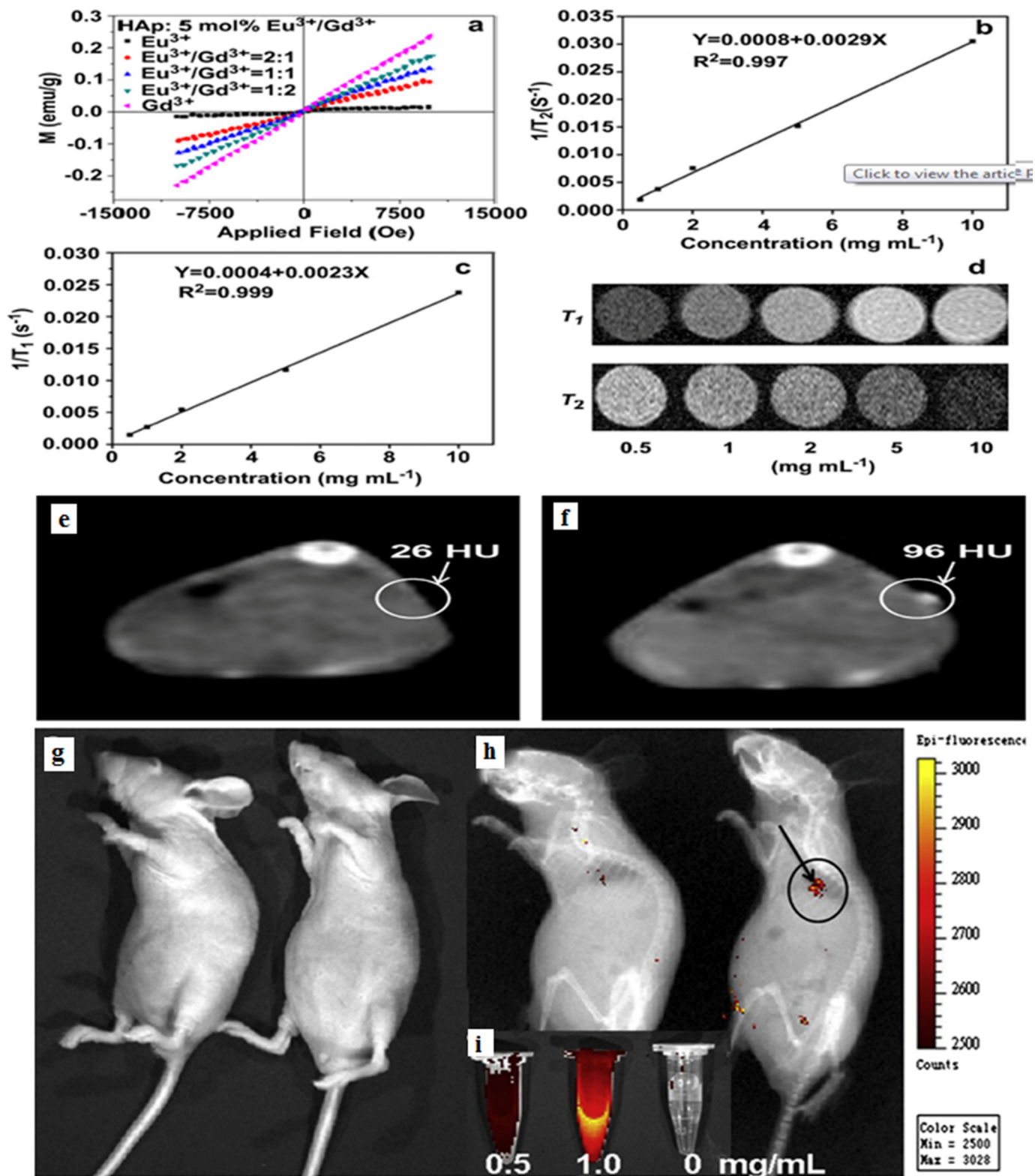


Fig. 15. (a) TEM image of  $\text{Fe}_3\text{O}_4$  –  $\text{SiO}_2$  – SrHAP microspheres; (b) Effect of pH on the immobilization capacity of microspheres towards  $\text{Pb}^{2+}$  ions; (c) Effect of contact time on  $\text{Pb}^{2+}$  immobilization (d) Effect of initial concentration on  $\text{Pb}^{2+}$  immobilization. Reprinted with the permission of [102]. Copyright (2014) American Chemical Society.



and luminescence was shown by  $\text{Eu}^{3+}$  concentration in designed composites with HAp. Moreover, these multifunctional MNCs had drug-releasing ability proved by a diffusion process. Results presented the

potential of  $\text{Eu}^{3+}$ - $\text{Gd}^{3+}$  co-doped HAp NCs in MRI, photoluminescence and computed tomography (Fig. 16). Imaging results before and after the injection clearly demonstrated the diagnostic ability of MRI, PL,



**Fig. 16.** (a) The magnetization loops of  $\text{Eu}^{3+}/\text{Gd}^{3+}$ -HAp nanorods; (b, c)  $T_2$  and  $T_1$  relaxivity of  $\text{Eu}^{3+}/\text{Gd}^{3+}$ -HAp nanorods; (d)  $T_1$  and  $T_2$  weighted CT images of  $\text{Eu}^{3+}/\text{Gd}^{3+}$ -HAp nanorods aqueous dispersed with various concentrations. (e, f) *In vivo* MR images of the nude mouse before and after injection with  $\text{Eu}^{3+}/\text{Gd}^{3+}$ -HAp ( $\text{Eu}^{3+}/\text{Gd}^{3+} = 1:2$ ). (g, h) *In vivo* PL imaging of the mice before and after subcutaneous injection of nanorods. (i) PL emission images of  $\text{Eu}^{3+}/\text{Gd}^{3+}$ -HAp nanorods at different concentrations. The excitation wavelength was 430 nm. Reprinted with the permission of [118]. Copyright (2011) Elsevier Ltd.

and CT techniques, enhanced using magnetic materials with HAp [118]. There are some other reports also which revealed that magnetic HAp NCs possess high magnetic moments which are suitable for magnetic resonance imaging [119,120].

In a recent work,  $\text{Dy}^{3+}$  and  $\text{Eu}^{3+}$  co-doped HAp were used for multimodal imaging (MRI, Photoluminescence).  $\text{Eu}^{3+}$  doped HAp showed the ability of photoluminescence and  $\text{Dy}^{3+}$  doped HAp possessed 5paramagnetic properties that lead to magnetic resonance imaging. Results showed the multimodal imaging of Dy-Eu-HAp co-doped composites [121].

The ability of magnetic HAp NCs to contribute to the field of biosensors as well as molecular imaging is clear. Due to the high photoelectric activity, fast transfer of electrons, high surface/volume ratio and selectivity of the magnetic HAp composites proved to be feasible for photochemical sensors, molecular imaging agents, and diagnostics in living systems.

### 3.8. Fire resistance

Fire-resistant paper-wood based materials are very important types of materials widely used in daily life. Hydroxyapatite based papers has shown excellent fire retardant ability [122]. Few reports were described the magnetic HAp NCs having fire resistance, magnetic, recyclable, superhydrophobic and environmentally friendly abilities. Magnetic  $\text{Ln}^{3+}$  doped HAp nanowires were reported based on composite paper having fire resistance, luminescent and waterproof properties. Furthermore, the composite paper showed flexibility, excellent process ability and tunable colour emission, and the pattern on the paper can be visible under UV light. Moreover, the composite paper represented a preservative ability even in fire and soaking in water [123]. In an alternative report, the manufacturing of thermally stable, fire-resistant, porous and permeable large-sized paper by using  $\text{Fe}_3\text{O}_4$ -HAp ultralong nanowires was reported. Moreover, the oil collecting device (mini boat) was made by this fire-resistant and permeable paper and was driven

magnetically in the oil-polluted region. The results indicated the selectivity of separation about >99.0%, permeation flux about  $2924.3 \text{ Lm}^{-2} \text{ h}^{-1}$ , and the ability of recycling was minimum 10 times. Fire resistance test was performed in comparison to the common paper and  $\text{HAp@Fe}_3\text{O}_4$ @PDMS paper gave excellent results even burning for 2 min (Fig. 17). These results verified the efficiency of magnetic HAp NCs paper as fire retardant, oil spillage treatment and survival of marine life [124].

Another study was reported regarding formation of fire-resistant magnetic wood using  $\text{CoFe}_2\text{O}_4$ -HAp NCs. The mechanical performance, magnetic ability, thermal behaviour and UV resistance were investigated experimentally. The outcomes predicted the use of  $\text{CoFe}_2\text{O}_4$ -HAp NCs modified magnetic wood in adsorption of heavy metals and electromagnetic waves as well as fire-resistant materials [125].

From these studies, it is proved that magnetic HAp NCs possess excellent fire-resistant properties and can be used in heat resistant devices and fire-retardant materials.

## 4. Conclusion and future prospective

Composite nanoparticles possess fascinating and unique characteristics owing to their hybrid nature, which expand their use in potential applications particularly in bio-nanotechnology. Nanomaterials of hydroxyapatite, magnetic materials have had prime attention of the biomaterial research society in recent decades. The ability to facilitate different ion-substitution into HAp has promoted design of new multifunctional and dual responsive nanomaterials for the betterment of biomaterials. This review presents important features of multidimensional ongoing research work on MHAp NCs which rarely have been reported before.

After the precise introduction of both materials, we have reviewed the various synthesis approaches such as hydrothermal, chemical precipitation, mechanochemical, emulsion synthesis, and template processes to substitute the magnetic component into the HAp configuring

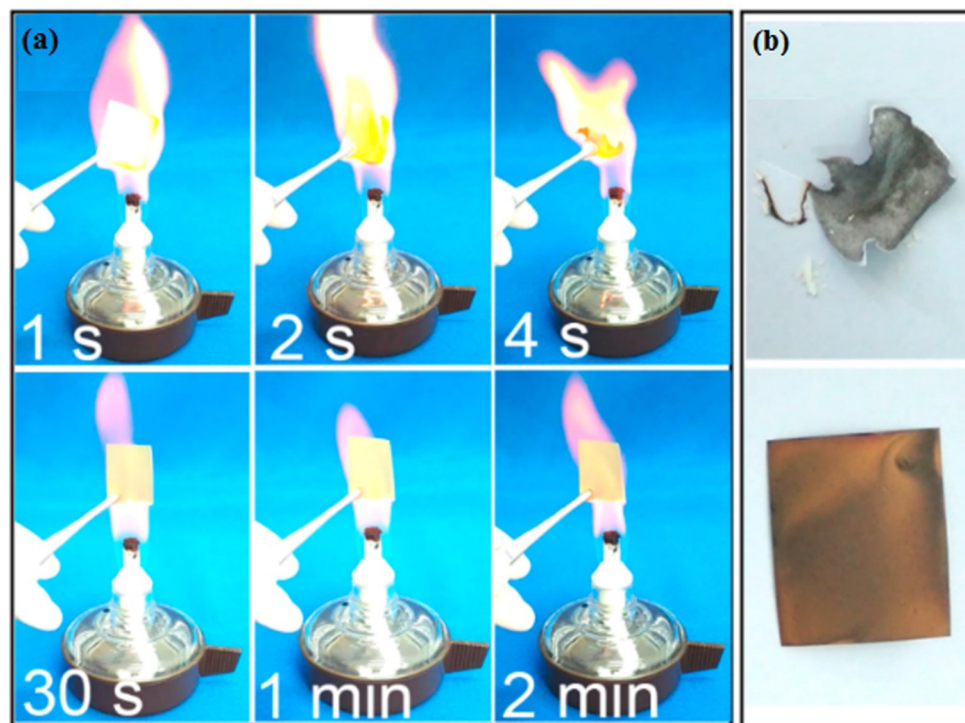


**Fig. 17.** (a) First row shows the fire-resistance tests of the common cellulose printing paper and second row illustrates the  $\text{HAp@Fe}_3\text{O}_4$ @PDMS paper. (b) Digital images of the common cellulose printing paper (first row) and the  $\text{HAp@Fe}_3\text{O}_4$ @PDMS paper (second row) after the fire resistance test. Reprinted with the permission of [124]. Copyright (2018) American Chemical Society.

MHAp NCs. Hydrothermal and modern template methods are suitable for the synthesis of nano MHAp materials with good control over shape and size as compared to other fabrication methods. It was also observed that synergetic techniques, combination of various synthetic routes, have promoted a better capability to regulate chemical compositions, dimensions and morphology of the MHAp nanoparticles. Although many reports have been available on the synthesis of MHAp there is plenty of room for improvement. The homogeneous formation of MHAp nanocrystals with controlled shape (core-shell) and size is required to be improved for commercialization of MHAp nanoparticles. Also, growth mechanism and a comprehensive study about the composite structure formation of MHAp is still in its infancy.

The excellent biocompatibility of these materials has made them promising for numerous medical applications but only few studies have been presented. Magnetic nanoparticles incorporated with HAp significantly increased the activity of HAp in regenerative implants. The drug loading/unloading ability of MHAp can be directly monitored by magnetic resonance imaging and improved the delivery under pH control. The MHAp NCs also showed exciting potential in detection or magnetic separation and cell labeling. The adsorption of heavy metal ion increased using MHAp rather than individual HAp because of superparamagnetic component in HAp. There are still many challenges such as rapid aggregation of particles, structure property relationship, long term safety, and critical evaluation *in vitro* (cell-particles interaction) and *in vivo* are required to attain the commercialization chances in the medical sector. The appropriate coating of HAp onto the magnetic nanoparticles or magnetic coating over HAp is highly desired to provide extensive advantages such as distinct surface functionalities to link various drugs and antibodies, protection from aggregation, and pH responsive nano MHAp assembly. Overall, we believe that MHAp-based diagnostics and therapeutics will make an exciting contribution in next generation medicine.

### CRedit authorship contribution statement

**Asim Mushtaq:** Visualization, Formal analysis, Investigation, Methodology, Data curation, Writing - original draft. **Ruibao Zhao:** Visualization, Formal analysis, Data curation. **Dandan Luo:** Visualization, Formal analysis, Data curation. **Eithne Dempsey:** Visualization, Methodology, Writing - review & editing. **Xiumei Wang:** Visualization, Methodology, Writing - review & editing. **M. Zubair Iqbal:** Conceptualization, Investigation, Funding acquisition, Methodology, Project administration, Supervision, Validation, Visualization, Writing - review & editing. **Xiangdong Kong:** Conceptualization, Investigation, Funding acquisition, Methodology, Project administration, Supervision, Validation, Visualization, Writing - review & editing.

### Declaration of Competing Interest

The authors declare that they have no known competing financial interests or personal relationships that could have appeared to influence the work reported in this paper.

### Acknowledgement

The authors acknowledge the support of National Natural Science Foundation of China (81950410638, 51672250, 51902289), Key Research and Development Program of Zhejiang Province (2019C04020) and Zhejiang Top Priority Discipline of Textile Science and Engineering 2017YBZX05).

### References

- [1] A.H. Lu, W. Schmidt, N. Matoussevitch, H. Bönemann, B. Spliethoff, B. Tesche, E. Bill, W. Kiefer, F. Schüth, Nanoengineering of a magnetically separable hydrogenation catalyst, *Angew. Chemie - Int. Ed.* 43 (2004) 4303–4306, <https://doi.org/10.1002/anie.200454222>.
- [2] L. He, M. Wang, J. Ge, Y. Yin, Magnetic assembly route to colloidal responsive photonic nanostructures, *Acc. Chem. Res.* 45 (2012) 1431–1440, <https://doi.org/10.1021/ar200276t>.
- [3] B. Gleich, J. Weizencker, Tomographic imaging using the nonlinear response of magnetic particles, *Nature.* 435 (2005) 1214–1217, <https://doi.org/10.1038/nature03808>.
- [4] J. Philip, P.D. Shima, B. Raj, Nanofluid with tunable thermal properties, *Appl. Phys. Lett.* 92 (2008) 10–13, <https://doi.org/10.1063/1.2838304>.
- [5] T. Hyeon, Chemical synthesis of magnetic nanoparticles, *Chem. Commun.* 3 (2003) 927–934, <https://doi.org/10.1039/b207789b>.
- [6] V. Mahendran, J. Philip, Nanofluid based optical sensor for rapid visual inspection of defects in ferromagnetic materials, *Appl. Phys. Lett.* 100 (2012) 51–54, <https://doi.org/10.1063/1.3684969>.
- [7] J. Philip, T. Jaykumar, P. Kalyanasundaram, B. Raj, A tunable optical filter, *Meas. Sci. Technol.* 14 (2003) 1289–1294, <https://doi.org/10.1088/0957-0233/14/8/314>.
- [8] D.W. Elliott, W.X. Zhang, Field assessment of nanoscale bimetallic particles for groundwater treatment, *Environ. Sci. Technol.* 35 (2001) 4922–4926, <https://doi.org/10.1021/es0108584>.
- [9] X. Li, J. Wei, K.E. Aifantis, Y. Fan, Q. Feng, F.Z. Cui, F. Watari, Current investigations into magnetic nanoparticles for biomedical applications, *J. Biomed. Mater. Res. A.* 104 (2016) 1285–1296, <https://doi.org/10.1002/jbm.a.35654>.
- [10] E. Peng, E.S.G. Choo, P. Chandrasekharan, C.T. Yang, J. Ding, K.H. Chuang, J.M. Xue, Synthesis of manganese ferrite/graphene oxide nanocomposites for biomedical applications, *Small.* 8 (2012) 3620–3630, <https://doi.org/10.1002/sml.201201427>.
- [11] H. Kaur, J. Singh, B.S. Randhawa, Essence of superparamagnetism in cadmium ferrite induced by various organic fuels via novel solution combustion method, *Ceram. Int.* 40 (2014) 12235–12243, <https://doi.org/10.1016/j.ceramint.2014.04.067>.
- [12] C.H. Hou, S.M. Hou, Y.S. Hsueh, J. Lin, H.C. Wu, F.H. Lin, The *in vivo* performance of biomagnetic hydroxyapatite nanoparticles in cancer hyperthermia therapy, *Biomaterials.* 30 (2009) 3956–3960, <https://doi.org/10.1016/j.biomaterials.2009.04.020>.
- [13] M.A. Hahn, A.K. Singh, P. Sharma, S.C. Brown, B.M. Moudgil, Nanoparticles as contrast agents for in-vivo bioimaging: current status and future perspectives, *Anal. Bioanal. Chem.* 399 (2011) 3–27, <https://doi.org/10.1007/s00216-010-4207-5>.
- [14] F. Miculescu, A. Maidaniuc, S.I. Voicu, V.K. Thakur, G.E. Stan, L.T. Ciocan, Progress in hydroxyapatite-starch based sustainable biomaterials for biomedical bone substitution applications, *ACS Sustain. Chem. Eng.* 5 (2017) 8491–8512, <https://doi.org/10.1021/acssuschemeng.7b02314>.
- [15] Y. Lu, W. Dong, J. Ding, W. Wang, A. Wang, Hydroxyapatite Nanomaterials: Synthesis, Properties, and Functional Applications, Elsevier Inc, 2019, <https://doi.org/10.1016/b978-0-12-814533-3.00010-7>.
- [16] S.R. Bakshi, D. Lahiri, A. Agarwal, Carbon nanotube reinforced metal matrix composites - a review, *Int. Mater. Rev.* 55 (2010) 41–64, <https://doi.org/10.1179/095066009X12572530170543>.
- [17] R. Morrissey, L.M. Rodríguez-Lorenzo, K.A. Gross, Influence of ferrous iron incorporation on the structure of hydroxyapatite, *J. Mater. Sci. Mater. Med.* 16 (2005) 387–392, <https://doi.org/10.1007/s10856-005-6976-5>.
- [18] M. Mahdavi, M. Bin Ahmad, M.J. Haron, F. Namvar, B. Nadi, M.Z. Ab Rahman, J. Amin, Synthesis, surface modification and characterisation of biocompatible magnetic iron oxide nanoparticles for biomedical applications, *Molecules.* 18 (2013) 7533–7548, <https://doi.org/10.3390/molecules18077533>.
- [19] A.M. El-Toni, M.A. Habila, J.P. Labis, Z.A. Althoshan, M. Alhoshan, A.A. Elzatahry, F. Zhang, Design, synthesis and applications of core-shell, hollow core, and nanorattle multifunctional nanostructures, *Nanoscale.* 8 (2016) 2510–2531, <https://doi.org/10.1039/c5nr07004j>.
- [20] J. Kim, H.S. Kim, N. Lee, T. Kim, H. Kim, T. Yu, I.C. Song, W.K. Moon, T. Hyeon, Multifunctional uniform nanoparticles composed of a magnetite nanocrystal core and a mesoporous silica shell for magnetic resonance and fluorescence imaging and for drug delivery, *Angew. Chemie - Int. Ed.* 47 (2008) 8438–8441, <https://doi.org/10.1002/anie.200802469>.
- [21] Y.P. Guo, T. Long, S. Tang, Y.J. Guo, Z.A. Zhu, Hydrothermal fabrication of magnetic mesoporous carbonated hydroxyapatite microspheres: biocompatibility, osteoinductivity, drug delivery property and bactericidal property, *J. Mater. Chem. B* 2 (2014) 2899–2909, <https://doi.org/10.1039/c3tb21829e>.
- [22] J.K. Sahoo, M. Konar, J. Rath, D. Kumar, H. Sahoo, Magnetic hydroxyapatite nanocomposite: impact on eriochrome black-T removal and antibacterial activity, *J. Mol. Liq.* 294 (2019) 111596, <https://doi.org/10.1016/j.molliq.2019.111596>.
- [23] F. Zhuang, R. Tan, W. Shen, X. Zhang, W. Xu, W. Song, Monodisperse magnetic hydroxyapatite/Fe<sub>3</sub>O<sub>4</sub> microspheres for removal of lead(II) from aqueous solution, *J. Alloys Compd.* 637 (2015) 531–537, <https://doi.org/10.1016/j.jallcom.2015.02.216>.
- [24] V. Sarath Chandra, K. Elayaraja, K. Thanigai Arul, S. Ferraris, S. Spriano, M. Ferraris, K. Asokan, S. Narayana Kalkura, Synthesis of magnetic hydroxyapatite by hydrothermal-microwave technique: dielectric, protein adsorption, blood compatibility and drug release studies, *Ceram. Int.* 41 (2015) 13153–13163, <https://doi.org/10.1016/j.ceramint.2015.07.088>.
- [25] Z. Stojanović, L. Veselinović, S. Marković, N. Ignjatović, D. Uskoković, Hydrothermal synthesis of nanosized pure and cobalt-exchanged hydroxyapatite, *Mater. Manuf. Process.* 24 (2009) 1096–1103, <https://doi.org/10.1080/10426910903032113>.
- [26] W. Chen, T. Long, Y.J. Guo, Z.A. Zhu, Y.P. Guo, Magnetic hydroxyapatite coatings with oriented nanorod arrays: hydrothermal synthesis, structure and biocompatibility, *J. Mater. Chem. B* 2 (2014) 1653–1660, <https://doi.org/10.1039/c3tb21769h>.
- [27] Y. Liu, Y. Sun, C. Cao, Y. Yang, Y. Wu, D. Ju, F. Li, Long-term biodistribution *in vivo* and toxicity of radioactive/magnetic hydroxyapatite nanorods, *Biomaterials.* 35 (2014) 3348–3355, <https://doi.org/10.1016/j.biomaterials.2013.12.064>.
- [28] Y.P. Guo, L.H. Guo, Y.B. Yao, C.Q. Ning, Y.J. Guo, Magnetic mesoporous carbonated hydroxyapatite microspheres with hierarchical nanostructure for drug delivery

- systems, *Chem. Commun.* 47 (2011) 12215–12217, <https://doi.org/10.1039/c1cc15190h>.
- [29] K. Lin, L. Chen, P. Liu, Z. Zou, M. Zhang, Y. Shen, Y. Qiao, X. Liu, J. Chang, Hollow magnetic hydroxyapatite microspheres with hierarchically mesoporous microstructure for pH-responsive drug delivery, *CrystEngComm* 15 (2013) 2999–3008, <https://doi.org/10.1039/c3ce26683d>.
- [30] S. Murakami, T. Hosono, B. Jeyadevan, M. Kamitakahara, K. Ioku, Hydrothermal synthesis of magnetite/hydroxyapatite composite material for hyperthermia therapy for bone cancer, *J. Ceram. Soc. Japan* 116 (2008) 950–954, <https://doi.org/10.2109/jcersj2.116.950>.
- [31] S. Periyasamy, V. Gopalakannan, N. Viswanathan, Hydrothermal assisted magnetic nano-hydroxyapatite encapsulated alginate beads for efficient Cr(VI) uptake from water, *J. Environ. Chem. Eng.* 6 (2018) 1443–1454, <https://doi.org/10.1016/j.jece.2018.01.007>.
- [32] I. Ullah, W. Zhang, L. Yang, M.W. Ullah, O.M. Atta, S. Khan, B. Wu, T. Wu, X. Zhang, Impact of structural features of Sr/Fe co-doped HAp on the osteoblast proliferation and osteogenic differentiation for its application as a bone substitute, *Mater. Sci. Eng. C* 110 (2020) 110633, <https://doi.org/10.1016/j.msec.2020.110633>.
- [33] I. Ullah, A. Gloria, W. Zhang, M.W. Ullah, B. Wu, W. Li, M. Domingos, X. Zhang, Synthesis and characterization of sintered Sr/Fe-modified hydroxyapatite bioceramics for bone tissue engineering applications, *ACS Biomater. Sci. Eng.* 6 (2020) 375–388, <https://doi.org/10.1021/acsbmaterials.9b01666>.
- [34] J.A. Ramos-guivar, M.A. Morales, F.J. Litterst,  $\gamma$ -Fe<sub>2</sub>O<sub>3</sub> nanoparticles embedded in nanohydroxyapatite matrix for magnetic hyperthermia and *in vitro* osteoblast cell studies, *Ceram. Int.* 46 (2020) 10658–10666, <https://doi.org/10.1016/j.ceramint.2020.01.072>.
- [35] Q. Wang, Y. Tang, Q. Ke, Q. Ke, W. Yin, C. Zhang, Y. Guo, J. Guan, Magnetic lanthanum-doped hydroxyapatite/chitosan scaffolds with endogenous stem cell-recruiting and immunomodulatory properties for bone regeneration, *J. Mater. Chem. B* 8 (2020) 5280–5292, <https://doi.org/10.1039/d0tb00342e>.
- [36] A. Vahdat, B. Ghasemi, M. Yousefpor, Synthesis of hydroxyapatite and hydroxyapatite/Fe<sub>3</sub>O<sub>4</sub> nanocomposite for removal of heavy metals, *Environ. Nanotechnology, Monit. Manag.* 12 (2019) 100233, <https://doi.org/10.1016/j.enmm.2019.100233>.
- [37] W. Sun, W. Jiang, G. Zhu, Y. Li, Magnetic CuO@HAP@ $\gamma$ -Fe<sub>2</sub>O<sub>3</sub> nanoparticles: an efficient catalyst for one-pot three-component reaction for the synthesis of imidazo [1,2-a]pyridines, *J. Organomet. Chem.* 873 (2018) 91–100, <https://doi.org/10.1016/j.jorganchem.2018.07.039>.
- [38] X. Xiao, L. Yang, D. Zhou, J. Zhou, Y. Tian, C. Song, C. Liu, Magnetic  $\gamma$ -Fe<sub>2</sub>O<sub>3</sub>/Fe-doped hydroxyapatite nanostructures as high-efficiency cadmium adsorbents, *Colloids Surfaces A Physicochem. Eng. Asp.* 555 (2018) 548–557, <https://doi.org/10.1016/j.colsurfa.2018.07.036>.
- [39] S. Mortazavi-Derazkola, M. Salavati-Niasari, H. Khojasteh, O. Amiri, S.M. Ghoreishi, Green synthesis of magnetic Fe<sub>3</sub>O<sub>4</sub>/SiO<sub>2</sub>/HAp nanocomposite for atenolol delivery and *in vivo* toxicity study, *J. Clean. Prod.* 168 (2017) 39–50, <https://doi.org/10.1016/j.jclepro.2017.08.235>.
- [40] N. Wakiya, M. Yamasaki, T. Adachi, A. Inukai, N. Sakamoto, D. Fu, O. Sakurai, K. Shinozaki, H. Suzuki, Preparation of hydroxyapatite-ferrite composite particles by ultrasonic spray pyrolysis, *Mater. Sci. Eng. B Solid-State Mater. Adv. Technol.* 173 (2010) 195–198, <https://doi.org/10.1016/j.mseb.2009.12.013>.
- [41] Z.P. Yang, X.Y. Gong, C.J. Zhang, Recyclable Fe<sub>3</sub>O<sub>4</sub>/hydroxyapatite composite nanoparticles for photocatalytic applications, *Chem. Eng. J.* 165 (2010) 117–121, <https://doi.org/10.1016/j.cej.2010.09.001>.
- [42] K.H. Zuo, Y.P. Zeng, D. Jiang, Synthesis and magnetic property of iron ions-doped hydroxyapatite, *J. Nanosci. Nanotechnol.* 12 (2012) 7096–7100, <https://doi.org/10.1166/jnn.2012.6578>.
- [43] W. Pon-On, S. Meejoo, I.M. Tang, Substitution of manganese and iron into hydroxyapatite: Core/shell nanoparticles, *Mater. Res. Bull.* 43 (2008) 2137–2144, <https://doi.org/10.1016/j.materresbull.2007.09.004>.
- [44] A. Safaei, F. Esmaeilzadeh, A. Sardarian, S.M. Mousavi, X. Wang, Experimental investigation of wettability alteration of carbonate gas-condensate reservoirs from oil-wetting to gas-wetting using Fe<sub>3</sub>O<sub>4</sub> nanoparticles coated with poly (vinyl alcohol), (PVA) or hydroxyapatite (HAP), *J. Pet. Sci. Eng.* 184 (2020) 106530, <https://doi.org/10.1016/j.petrol.2019.106530>.
- [45] N. Petchsang, W. Pon-On, J.H. Hodak, I.M. Tang, Magnetic properties of co-ferrite-doped hydroxyapatite nanoparticles having a core/shell structure, *J. Magn. Magn. Mater.* 321 (2009) 1990–1995, <https://doi.org/10.1016/j.jmmm.2008.12.027>.
- [46] H. Wu, Q. Li, Application of mechanochemical synthesis of advanced materials, *J. Adv. Ceram.* 1 (2012) 130–137, <https://doi.org/10.1007/s40145-012-0012-2>.
- [47] X. Chunping, D. Sudipta, M.B. Alina, O. Manuel, L. Rafael, Mechanochemical synthesis of advanced nanomaterials for catalytic applications Chunping, *Chem. Commun.* (2015) 6698–6713, <https://doi.org/10.1039/C4CC09876E>.
- [48] A. Fahami, B. Nasiri-Tabrizi, Characterization of mechanochemical-synthesized hydroxyapatite-magnesium titanate composite nanopowders, *J. Adv. Ceram.* 2 (2013) 63–70, <https://doi.org/10.1007/s40145-013-0043-3>.
- [49] A. Fahami, R. Ebrahimi-Kahrizangi, B. Nasiri-Tabrizi, Mechanochemical synthesis of hydroxyapatite/titanium nanocomposite, *Solid State Sci.* 13 (2011) 135–141, <https://doi.org/10.1016/j.solidstsciences.2010.10.026>.
- [50] A. Fahami, B. Nasiri-Tabrizi, R. Ebrahimi-Kahrizangi, Synthesis of calcium phosphate-based composite nanopowders by mechanochemical process and subsequent thermal treatment, *Ceram. Int.* 38 (2012) 6729–6738, <https://doi.org/10.1016/j.ceramint.2012.05.064>.
- [51] T. Iwasaki, R. Nakatsuka, K. Murase, H. Takata, H. Nakamura, S. Watano, Simple and rapid synthesis of magnetite/hydroxyapatite composites for hyperthermia treatments via a mechanochemical route, *Int. J. Mol. Sci.* 14 (2013) 9365–9378, <https://doi.org/10.3390/ijms14059365>.
- [52] M. Sneha, N.M. Sundaram, Preparation and characterization of an iron oxide-hydroxyapatite nanocomposite for potential bone cancer therapy, *Int. J. Nanomedicine* 10 (2015) 99–106, <https://doi.org/10.2147/IJN.S79985>.
- [53] Q. Zhang, S. Dan, K. Du, Fabrication and characterization of magnetic hydroxyapatite entrapped Agarose composite beads with high adsorption capacity for heavy metal removal, *Ind. Eng. Chem. Res.* 56 (2017) 8705–8712, <https://doi.org/10.1021/acs.iecr.7b01635>.
- [54] F. Foroughi, S.A. Hassanzadeh-Tabrizi, J. Amighian, Microemulsion synthesis and magnetic properties of hydroxyapatite-encapsulated nano CoFe<sub>2</sub>O<sub>4</sub>, *J. Magn. Magn. Mater.* 382 (2015) 182–187, <https://doi.org/10.1016/j.jmmm.2015.01.075>.
- [55] M. Iafisco, M. Sandri, S. Panseri, J.M. Delgado-López, J. Gómez-Morales, A. Tampieri, Magnetic bioactive and biodegradable hollow Fe-doped hydroxyapatite coated poly(l-lactic) acid micro-nanospheres, *Chem. Mater.* 25 (2013) 2610–2617, <https://doi.org/10.1021/cm4007298>.
- [56] Y. Xie, D. Kocafe, C. Chen, Y. Kocafe, Review of research on template methods in preparation of nanomaterials, *J. Nanomater* 2016 (2016) 1–10, <https://doi.org/10.1155/2016/2302595>.
- [57] J. Liu, Y. Liu, Y. Kong, J. Yao, Y. Cai, Formation of vaterite regulated by silk sericin and its transformation towards hydroxyapatite microsphere, *Mater. Lett.* 110 (2013) 221–224, <https://doi.org/10.1016/j.matlet.2013.08.021>.
- [58] W. Pon-On, N. Charoenphandhu, I.M. Tang, P. Jongwattanapisan, N. Krishnamra, R. Hoonsawat, Encapsulation of magnetic CoFe<sub>2</sub>O<sub>4</sub> in SiO<sub>2</sub> nanocomposites using hydroxyapatite as templates: a drug delivery system, *Mater. Chem. Phys.* 131 (2011) 485–494, <https://doi.org/10.1016/j.matchemphys.2011.10.008>.
- [59] A. Mir, D. Mallik, S. Bhattacharyya, D. Mahata, A. Sinha, S. Nayar, Aqueous ferrofluids as templates for magnetic hydroxyapatite nanocomposites, *J. Mater. Sci. Mater. Med.* 21 (2010) 2365–2369, <https://doi.org/10.1007/s10856-010-4090-9>.
- [60] R.K. Singh, A.M. El-Fiqi, K.D. Patel, H.W. Kim, A novel preparation of magnetic hydroxyapatite nanotubes, *Mater. Lett.* 75 (2012) 130–133, <https://doi.org/10.1016/j.matlet.2012.01.129>.
- [61] H.R. Ali, H.H. El-Maghrabi, F. Zahran, Y.M. Moustafa, A novel surface imprinted polymer/magnetic hydroxyapatite nanocomposite for selective dibenzothiophene scavenging, *Appl. Surf. Sci.* 426 (2017) 56–66, <https://doi.org/10.1016/j.apsusc.2017.07.105>.
- [62] X. Cui, M.A. Green, P.J. Blower, D. Zhou, Y. Yan, W. Zhang, K. Djanashvili, D. Mathe, D.S. Veres, K. Sziget, Al(OH)<sub>3</sub> facilitated synthesis of water-soluble, magnetic, radiolabelled and fluorescent hydroxyapatite nanoparticles, *Chem. Commun.* 51 (2015) 9332–9335, <https://doi.org/10.1039/c5cc02259b>.
- [63] S. Mondal, P. Manivasagan, S. Bharathiraja, M.S. Moorthy, V.T. Nguyen, H.H. Kim, S.Y. Nam, K.D. Lee, J. Oh, Hydroxyapatite coated iron oxide nanoparticles: a promising nanomaterial for magnetic hyperthermia cancer treatment, *Nanomaterials* 7 (2017) 1–15, <https://doi.org/10.3390/nano7120426>.
- [64] Z. Xu, G. Huang, Z. Yan, N. Wang, L. Yue, Q. Liu, Hydroxyapatite-supported low-content Pt catalysts for efficient removal of formaldehyde at room temperature, *ACS Omega* 4 (2019) 21998–22007, <https://doi.org/10.1021/acsomega.9b03068>.
- [65] L. Gu, X. He, Z. Wu, Mesoporous Fe<sub>3</sub>O<sub>4</sub>/hydroxyapatite composite for targeted drug delivery, *Mater. Res. Bull.* 59 (2014) 65–68, <https://doi.org/10.1016/j.materresbull.2014.06.018>.
- [66] Y. Zhao, T. Fan, J. Chen, J. Su, X. Zhi, P. Pan, L. Zou, Q. Zhang, Magnetic bioinspired micro/nanostructured composite scaffold for bone regeneration, *Colloids Surfaces B Biointerfaces* 174 (2019) 70–79, <https://doi.org/10.1016/j.colsurfb.2018.11.003>.
- [67] Z. Abbasi, S. Rezaei, M. Bagheri, R. Hajinasiri, Preparation of a novel, efficient, and recyclable magnetic catalyst,  $\gamma$ -Fe<sub>2</sub>O<sub>3</sub>@HAP-Ag nanoparticles, and a solvent- and halogen-free protocol for the synthesis of coumarin derivatives, *Chinese Chem. Lett.* 28 (2017) 75–82, <https://doi.org/10.1016/j.ccllet.2016.06.022>.
- [68] S.Y. Srinivasan, K.M. Paknikar, V. Gajbhiye, D. Bodas, Magneto-conducting core/shell nanoparticles for biomedical applications, *ChemNanoMat* 4 (2018) 151–164, <https://doi.org/10.1002/cnma.201700278>.
- [69] W. Lai, C. Chen, X. Ren, I. Lee, G. Jiang, X. Kong, Hydrothermal fabrication of porous hollow hydroxyapatite microspheres for a drug delivery system, *Mater. Sci. Eng. C* 62 (2016) 166–172, <https://doi.org/10.1016/j.msec.2016.01.055>.
- [70] R. Zhao, X. Yang, C. Chen, K. Chen, S. Wang, C. Xie, X. Ren, X. Kong, The anti-tumor effect of p53 gene-loaded hydroxyapatite nanoparticles *in vitro* and *in vivo*, *J. Nanopart. Res.* 16 (2014) 2353, <https://doi.org/10.1007/s11051-014-2353-y>.
- [71] H. Yang, L. Hao, N. Zhao, C. Du, Y. Wang, Hierarchical porous hydroxyapatite microsphere as drug delivery carrier, *CrystEngComm* 15 (2013) 5760–5763, <https://doi.org/10.1039/c3ce40710a>.
- [72] J. Jin, G. Zuo, G. Xiong, H. Luo, Q. Li, C. Ma, D. Li, F. Gu, Y. Ma, Y. Wan, The inhibition of lamellar hydroxyapatite and lamellar magnetic hydroxyapatite on the migration and adhesion of breast cancer cells, *J. Mater. Sci. Mater. Med.* 25 (2014) 1025–1031, <https://doi.org/10.1007/s10856-013-5126-8>.
- [73] C.L. Tseng, K.C. Chang, M.C. Yeh, K.C. Yang, T.P. Tang, F.H. Lin, Development of a dual-functional Pt-Fe-HAP magnetic nanoparticles application for chemo-hyperthermia treatment of cancer, *Ceram. Int.* 40 (2014) 5117–5127, <https://doi.org/10.1016/j.ceramint.2013.09.137>.
- [74] B. Govindan, B.S. Latha, P. Nagamony, F. Ahmed, M.A. Saifi, A.H. Harrath, S. Alwasel, L. Mansour, E.H. Alsharaeh, Designed synthesis of nanostructured magnetic hydroxyapatite based drug nanocarrier for anti-cancer drug delivery toward the treatment of human epidermoid carcinoma, *Nanomaterials* 7 (2017) 1–16, <https://doi.org/10.3390/nano7060138>.
- [75] S. Xu, Z. Qiu, J. Wu, X. Kong, Osteogenic differentiation gene expression profiling of hMSCs on hydroxyapatite and mineralized collagen, *Tissue Eng. Part A* 22 (2015) 170–181.

- [76] L. Liu, J. Liu, X. Kong, Y. Cai, J. Yao, Porous composite scaffolds of hydroxyapatite / silk fibroin via two-step method, *Polym. Adv. Technol.* 22 (2011) 909–914, <https://doi.org/10.1002/pat.1595>.
- [77] A. Gloria, R. De Santis, M. Uhlarz, A. Tampieri, J. Rivas, T. Herrmannsdörfer, V.A. Dediu, L.A. Ambrosio Gloria, T. Russo, S. Zepetelli, M. Sandri, M. Bañobre-López, Y. Piñero-Redondo, L. Ambrosio, Magnetic poly( $\epsilon$ -caprolactone)/iron-doped hydroxyapatite nanocomposite substrates for advanced bone tissue engineering, *J. R. Soc. Interface* 10 (2013) 1–11, <https://doi.org/10.1098/rsif.2012.0833>.
- [78] A. Tampieri, M. Iafisco, M. Sandri, S. Panseri, C. Cunha, S. Sprio, E. Savini, M. Uhlarz, T. Herrmannsdörfer, Magnetic bioinspired hybrid nanostructured collagen-hydroxyapatite scaffolds supporting cell proliferation and tuning regenerative process, *ACS Appl. Mater. Interfaces* 6 (2014) 15697–15707, <https://doi.org/10.1021/am5050967>.
- [79] H.C. Wu, T.W. Wang, M.C. Bohn, F.H. Lin, M. Spector, Novel magnetic hydroxyapatite nanoparticles as non-viral vectors for the glial cell line-derived neurotrophic factor gene, *Adv. Funct. Mater.* 20 (2010) 67–77, <https://doi.org/10.1002/adfm.200901108>.
- [80] P. Chen, L. Liu, J. Pan, J. Mei, C. Li, Y. Zheng, Biomimetic composite scaffold of hydroxyapatite/gelatin-chitosan core-shell nanofibers for bone tissue engineering, *Mater. Sci. Eng. C* 97 (2019) 325–335, <https://doi.org/10.1016/j.msec.2018.12.027>.
- [81] Q. Zhong, W. Li, X. Su, G. Li, Y. Zhou, S.C. Kundu, J. Yao, Y. Cai, Degradation pattern of porous CaCO<sub>3</sub> and hydroxyapatite microspheres *in vitro* and *in vivo* for potential application in bone tissue engineering, *Colloids Surfaces B Biointerfaces* 143 (2016) 56–63, <https://doi.org/10.1016/j.colsurfb.2016.03.020>.
- [82] C. Gao, Y. Cai, X. Kong, G. Han, J. Yao, Development and characterization of injectable chitosan-based hydrogels containing dexamethasone / rhBMP-2 loaded hydroxyapatite nanoparticles, *Mater. Lett.* 93 (2013) 312–315, <https://doi.org/10.1016/j.matlet.2012.11.106>.
- [83] M. Pan, X. Kong, Y. Cai, J. Yao, Hydroxyapatite coating on the titanium substrate modulated by a recombinant collagen-like protein, *Mater. Chem. Phys.* 126 (2011) 811–817, <https://doi.org/10.1016/j.matchemphys.2010.12.037>.
- [84] Y. Cai, J. Yu, S.C. Kundu, J. Yao, Multifunctional nano-hydroxyapatite and alginate / gelatin based sticky gel composites for potential bone regeneration, *Mater. Chem. Phys.* 181 (2016) 227–233, <https://doi.org/10.1016/j.matchemphys.2016.06.053>.
- [85] S. Panseri, C. Cunha, T. D'Alessandro, M. Sandri, G. Giavaresi, M. Marcacci, C.T. Hung, A. Tampieri, Intrinsically superparamagnetic Fe-hydroxyapatite nanoparticles positively influence osteoblast-like cell behaviour, *J. Nanobiotechnology* 10 (2012) 1–10, <https://doi.org/10.1186/1477-3155-10-32>.
- [86] H. Koley, D.R. Howlader, U. Bhaumik, Assessment of Antimicrobial Activity of Different Phytochemicals against Enteric Diseases in Different Animal Models, Elsevier Inc., 2019 <https://doi.org/10.1016/b978-0-12-814619-4.00022-7>.
- [87] M. Turkoz, A.O. Atilla, Z. Evis, Silver and fluoride doped hydroxyapatites: investigation by microstructure, mechanical and antibacterial properties, *Ceram. Int.* 39 (2013) 8925–8931, <https://doi.org/10.1016/j.ceramint.2013.04.088>.
- [88] K. Kaviyarasu, A. Mariappan, K. Neyvasagam, A. Ayeshamariam, P. Pandi, R.R. Palanichamy, C. Gopinathan, G.T. Mola, M. Maaza, Photocatalytic performance and antimicrobial activities of HAP-TiO<sub>2</sub> nanocomposite thin films by sol-gel method, *Surfaces and Interfaces* 6 (2017) 247–255, <https://doi.org/10.1016/j.surfin.2016.10.002>.
- [89] A. Seyfoori, S.A.S. Ebrahimi, S. Omidian, S.M. Naghib, Multifunctional magnetic ZnFe<sub>2</sub>O<sub>4</sub>-hydroxyapatite nanocomposite particles for local anti-cancer drug delivery and bacterial infection inhibition: an *in vitro* study, *J. Taiwan Inst. Chem. Eng.* 96 (2019) 503–508, <https://doi.org/10.1016/j.jtice.2018.10.018>.
- [90] M.A. Morsi, A.E.M. Hezma, Effect of iron doped hydroxyapatite nanoparticles on the structural, morphological, mechanical and magnetic properties of polylactic acid polymer, *J. Mater. Res. Technol.* 8 (2019) 2098–2106, <https://doi.org/10.1016/j.jmrt.2019.01.017>.
- [91] J.P. Adams, M.J.B. Brown, A. Diaz-Rodríguez, R.C. Lloyd, G.D. Roiban, Biocatalysis: a pharma perspective, *Adv. Synth. Catal.* 361 (2019) 2421–2432, <https://doi.org/10.1002/adsc.201900424>.
- [92] W. Xie, X. Zang, Covalent immobilization of lipase onto aminopropyl-functionalized hydroxyapatite-encapsulated- $\gamma$ -Fe<sub>2</sub>O<sub>3</sub> nanoparticles: a magnetic biocatalyst for interesterification of soybean oil, *Food Chem.* 227 (2017) 397–403, <https://doi.org/10.1016/j.foodchem.2017.01.082>.
- [93] T.C. Coutinho, P.W. Tardioli, C.S. Farinas, Hydroxyapatite nanoparticles modified with metal ions for xylanase immobilization, *Int. J. Biol. Macromol.* 150 (2020) 344–353, <https://doi.org/10.1016/j.ijbiomac.2020.02.058>.
- [94] T. Yabutsuka, S. Kumazawa, D. Hisashuku, H. Mizutani, K. Fukushima, S. Takai, T. Yao, Enzyme immobilization by using apatite microcapsules with magnetic properties, *Key Eng. Mater.* 696 (2016) 259–264, <https://doi.org/10.4028/www.scientific.net/KEM.696.259>.
- [95] S. Saire-Saire, S. Garcia-Segura, C. Luyo, L.H. Andrade, H. Alarcon, Magnetic biocomposite catalysts of CoFe<sub>2</sub>O<sub>4</sub>/hydroxyapatite-lipase for enantioselective synthesis provide a framework for enzyme recovery and reuse, *Int. J. Biol. Macromol.* 148 (2020) 284–291, <https://doi.org/10.1016/j.ijbiomac.2020.01.137>.
- [96] M. Khoobi, M. Khalilvand-Sedagheh, A. Ramazani, Z. Asadgol, H. Forootanfar, M.A. Faramarzi, Synthesis of polyethyleneimine (PEI) and  $\beta$ -cyclodextrin grafted PEI nanocomposites with magnetic cores for lipase immobilization and esterification, *J. Chem. Technol. Biotechnol.* 91 (2016) 375–384, <https://doi.org/10.1002/jctb.4579>.
- [97] M. Sheykhan, L. Ma'Mani, A. Ebrahimi, A. Heydari, Sulfamic acid heterogenized on hydroxyapatite-encapsulated  $\gamma$ -Fe<sub>2</sub>O<sub>3</sub> nanoparticles as a magnetic green interphase catalyst, *J. Mol. Catal. A Chem.* 335 (2011) 253–261, <https://doi.org/10.1016/j.molcata.2010.12.004>.
- [98] A.G. Varghese, S.A. Paul, M.S. Latha, Remediation of heavy metals and dyes from wastewater using cellulose-based adsorbents, *Environ. Chem. Lett.* 17 (2019) 867–877, <https://doi.org/10.1007/s10311-018-00843-z>.
- [99] Y. Wang, L. Hu, G. Zhang, T. Yan, L. Yan, Q. Wei, B. Du, Removal of Pb(II) and methylene blue from aqueous solution by magnetic hydroxyapatite-immobilized oxidized multi-walled carbon nanotubes, *J. Colloid Interface Sci.* 494 (2017) 380–388, <https://doi.org/10.1016/j.jcis.2017.01.105>.
- [100] F. Piri, A. Mollahosseini, A. Khadir, M. Milani Hosseini, Enhanced adsorption of dyes on microwave-assisted synthesized magnetic zeolite-hydroxyapatite nanocomposite, *J. Environ. Chem. Eng.* 7 (2019) 103338, <https://doi.org/10.1016/j.jece.2019.103338>.
- [101] F. Zhang, B. Ma, X. Jiang, Y. Ji, Dual function magnetic hydroxyapatite nanopowder for removal of malachite green and Congo red from aqueous solution, *Powder Technol.* 302 (2016) 207–214, <https://doi.org/10.1016/j.powtec.2016.08.044>.
- [102] F.Q. Zhuang, R.Q. Tan, W.F. Shen, X.P. Zhang, W. Xu, W.J. Song, Magnetic strontium hydroxyapatite microspheres for the efficient removal of Pb(II) from acidic solutions, *J. Chem. Eng. Data* 59 (2014) 3873–3881, <https://doi.org/10.1021/je500763y>.
- [103] F. Foroughi, S.A. Hassanzadeh-Tabrizi, J. Amighian, A. Saffar-Teluri, A designed magnetic CoFe<sub>2</sub>O<sub>4</sub>-hydroxyapatite core-shell nanocomposite for Zn(II) removal with high efficiency, *Ceram. Int.* 41 (2015) 6844–6850, <https://doi.org/10.1016/j.ceramint.2015.01.133>.
- [104] P. Hou, C. Shi, L. Wu, X. Hou, Chitosan/hydroxyapatite/Fe<sub>3</sub>O<sub>4</sub> magnetic composite for metal-complex dye AY220 removal: recyclable metal-promoted Fenton-like degradation, *Microchem. J.* 128 (2016) 218–225, <https://doi.org/10.1016/j.microc.2016.04.022>.
- [105] A. Phasuk, S. Srisantitham, T. Tuntulani, W. Anutrakakda, Facile synthesis of magnetic hydroxyapatite-supported nickel oxide nanocomposite and its dye adsorption characteristics, *Adsorption* 24 (2018) 157–167, <https://doi.org/10.1007/s10450-017-9931-0>.
- [106] F. Zhang, X. Yin, W. Zhang, Y. Ji, Optimizing decolorization of methyl blue solution by two magnetic hydroxyapatite nanorods, *J. Taiwan Inst. Chem. Eng.* 65 (2016) 269–275, <https://doi.org/10.1016/j.jtice.2016.05.019>.
- [107] D.I. Cifci, Enhancement of Methylene Blue dye adsorption by Fe-Hydroxyapatite composite, *Adv. Environ. Res.* 5 (2016) 225–235, <https://doi.org/10.12989/aer.2016.5.4.225>.
- [108] J.B. Haun, T.J. Yoon, H. Lee, R. Weissleder, Magnetic nanoparticle biosensors, *Wiley Interdiscip. Rev. Nanomedicine Nanobiotechnology* 2 (2010) 291–304, <https://doi.org/10.1002/wnan.84>.
- [109] R. Weissleder, U. Mahmood, *Molecular imaging*, *Radiology* 219 (2001) 316–333.
- [110] S.S. Syamchand, G. Sony, Multifunctional hydroxyapatite nanoparticles for drug delivery and multimodal molecular imaging, *Microchim. Acta* 182 (2015) 1567–1589, <https://doi.org/10.1007/s00604-015-1504-x>.
- [111] Z. Li, Z. Liu, M. Yin, X. Yang, Q. Yuan, J. Ren, X. Qu, Aptamer-capped multifunctional mesoporous strontium hydroxyapatite nanovehicle for cancer-cell-responsive drug delivery and imaging, *Biomacromolecules* 13 (2012) 4257–4263, <https://doi.org/10.1021/bm301563q>.
- [112] R. Mirzajani, S. Karimi, Preparation of  $\gamma$ -Fe<sub>2</sub>O<sub>3</sub>/hydroxyapatite/Cu(II) magnetic nanocomposite and its application for electrochemical detection of metformin in urine and pharmaceutical samples, *Sensors Actuators B Chem.* 270 (2018) 405–416, <https://doi.org/10.1016/j.snb.2018.05.032>.
- [113] G. Jiang, L. Song, D. Tao, F. Jin, Characterization of luminescent hydroxyapatite@terbium complex core-shell composites using chlorobenzoic acid as ligands, *J. Rare Earths* (2019) <https://doi.org/10.1016/j.jre.2019.10.009>.
- [114] Z. Yang, X. Shang, C. Zhang, J. Zhu, Photoelectrochemical bilirubin biosensor based on Fe<sub>3</sub>O<sub>4</sub>/hydroxyapatite/molecularly imprinted polypyrrole nanoparticles, *Sensors Actuators B Chem.* 201 (2014) 167–172, <https://doi.org/10.1016/j.snb.2014.05.021>.
- [115] P. Kanchana, N. Lavanya, C. Sekar, Development of amperometric L-tyrosine sensor based on Fe-doped hydroxyapatite nanoparticles, *Mater. Sci. Eng. C* 35 (2014) 85–91, <https://doi.org/10.1016/j.msec.2013.10.013>.
- [116] L. Li, Y. Liu, J. Tao, M. Zhang, H. Pan, X. Xu, R. Tang, Surface modification of hydroxyapatite nanocrystallite by a small amount of terbium provides a biocompatible fluorescent probe, *J. Phys. Chem. C* 112 (2008) 12219–12224, <https://doi.org/10.1021/jp8026463>.
- [117] A. Ashokan, P. Chandran, A.R. Sadanandan, C.K. Koduri, A.P. Retnakumari, D. Menon, S. Nair, M. Koyakutty, Development and haematotoxicological evaluation of doped hydroxyapatite based multimodal nanocontrast agent for near-infrared, magnetic resonance and X-ray contrast imaging, *Nanotoxicology* 6 (2012) 652–666, <https://doi.org/10.3109/17435390.2011.600839>.
- [118] F. Chen, P. Huang, Y.J. Zhu, J. Wu, C.L. Zhang, D.X. Cui, The photoluminescence, drug delivery and imaging properties of multifunctional Eu<sup>3+</sup>/Gd<sup>3+</sup> dual-doped hydroxyapatite nanorods, *Biomaterials* 32 (2011) 9031–9039, <https://doi.org/10.1016/j.biomaterials.2011.08.032>.
- [119] M.S. Laranjeira, A. Moço, J. Ferreira, S. Coimbra, E. Costa, A. Santos-Silva, P.J. Ferreira, F.J. Monteiro, Different hydroxyapatite magnetic nanoparticles for medical imaging: its effects on hemostatic, hemolytic activity and cellular cytotoxicity, *Colloids Surfaces B Biointerfaces* 146 (2016) 363–374, <https://doi.org/10.1016/j.colsurfb.2016.06.042>.
- [120] F. Caseiro Alves, P. Donato, A.D. Sherry, A. Zaheer, S. Zhang, A.J.M. Lubag, M.E. Merritt, R.E. Lenkinski, J.V. Frangioni, M. Neves, M.I.M. Prata, A.C. Santos, J.J.P. De Lima, C.F.G.C. Geraldés, Silencing of phosphonate-gadolinium magnetic resonance imaging contrast by hydroxyapatite binding, *Investig. Radiol.* 38 (2003) 750–760, <https://doi.org/10.1097/01.rli.0000084891.15996.0f>.
- [121] A. Tesch, C. Wenisch, K.H. Herrmann, J.R. Reichenbach, P. Warncke, D. Fischer, F.A. Müller, Luminomagnetic Eu<sup>3+</sup>- and Dy<sup>3+</sup>-doped hydroxyapatite for multimodal imaging, *Mater. Sci. Eng. C* 81 (2017) 422–431, <https://doi.org/10.1016/j.msec.2017.08.032>.
- [122] S. Elbasuney, A. Maraden, Novel thermost nanocomposite intumescent coating based on hydroxyapatite Nanoplates for fireproofing of steel structures, *J. Inorg.*

- Organomet. Polym. Mater. 30 (2020) 820–830, <https://doi.org/10.1007/s10904-019-01260-7>.
- [123] R.L. Yang, Y.J. Zhu, F.F. Chen, L.Y. Dong, Z.C. Xiong, Luminescent, fire-resistant, and water-proof ultralong hydroxyapatite nanowire-based paper for multimode Anti-counterfeiting applications, ACS Appl. Mater. Interfaces 9 (2017) 25455–25464, <https://doi.org/10.1021/acsami.7b06835>.
- [124] R.L. Yang, Y.J. Zhu, F.F. Chen, D.D. Qin, Z.C. Xiong, Recyclable, fire-resistant, Superhydrophobic, and magnetic paper based on Ultralong hydroxyapatite nanowires for continuous oil/water separation and oil collection, ACS Sustain. Chem. Eng. 6 (2018) 10140–10150, <https://doi.org/10.1021/acssuschemeng.8b01463>.
- [125] W. Gan, L. Gao, X. Zhan, J. Li, Hydrothermal synthesis of magnetic wood composites and improved wood properties by precipitation with  $\text{CoFe}_2\text{O}_4$ /hydroxyapatite, RSC Adv. 5 (2015) 45919–45927, <https://doi.org/10.1039/c5ra06138e>.